

See discussions, stats, and author profiles for this publication at: <https://www.researchgate.net/publication/26883310>

Enantioselective Rhodium–Catalyzed [2+2+2] Cycloadditions of Terminal Alkynes and Alkenyl Isocyanates: Mechanistic Insights Lead to a Unified Model that Rationalizes Product Select...

ARTICLE in JOURNAL OF THE AMERICAN CHEMICAL SOCIETY · OCTOBER 2009

Impact Factor: 12.11 · DOI: 10.1021/ja905065j · Source: PubMed

CITATIONS

50

READS

17

9 AUTHORS, INCLUDING:



Kevin M Oberg

Colorado State University

14 PUBLICATIONS 311 CITATIONS

SEE PROFILE



Tomislav Rovis

Colorado State University

180 PUBLICATIONS 7,742 CITATIONS

SEE PROFILE

Published in final edited form as:

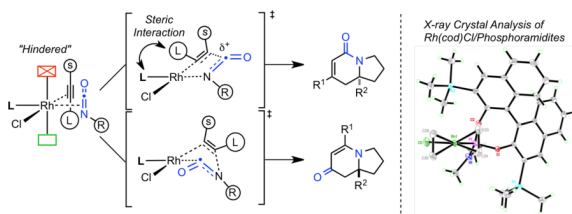
J Am Chem Soc. 2009 November 4; 131(43): 15717–15728. doi:10.1021/ja905065j.

Enantioselective Rhodium-Catalyzed [2+2+2] Cycloadditions of Terminal Alkynes and Alkenyl Isocyanates: Mechanistic Insights Lead to a Unified Model that Rationalizes Product Selectivity

Derek M. Dalton, Kevin M. Oberg, Robert T. Yu, Ernest E. Lee, Stéphane Perreault, Mark Emil Oinen, Melissa L. Pease, Guillaume Malik, and Tomislav Rovis*

Department of Chemistry, Colorado State University, Fort Collins, CO, 80523

Abstract



This manuscript describes the development and scope of the asymmetric rhodium-catalyzed [2+2+2] cycloaddition of terminal alkynes and alkenyl isocyanates leading to the formation of indolizidine and quinolizidine scaffolds. The use of phosphoramidite ligands proved crucial for avoiding competitive terminal alkyne dimerization. Both aliphatic and aromatic terminal alkynes participate well, with product selectivity a function of both the steric and electronic character of the alkyne. Manipulation of the phosphoramidite ligand leads to tuning of enantio- and product selectivity, with a complete turnover in product selectivity seen with aliphatic alkynes when moving from Taddol-based to biphenol-based phosphoramidites. Terminal and 1,1-disubstituted olefins are tolerated with nearly equal efficacy. Examination of a series of competition experiments in combination with analysis of reaction outcome shed considerable light on the operative catalytic cycle. Through a detailed study of a series of X-ray structures of rhodium(cod)chloride/phosphoramidite complexes, we have formulated a mechanistic hypothesis that rationalizes the observed product selectivity.

Keywords

Asymmetric Catalysis; [2+2+2] cycloaddition; Rhodium; Isocyanate; Alkyne; Alkene; Phosphoramidite

Introduction

Indolizidines and quinolizidines are common motifs found in many biologically active natural products isolated from arthropod, amphibian, plant, and marine sources (Figure 1).¹ Interest in the synthesis of these compounds is threefold: scarcity of natural sources, pharmacological activity, and unique structural features. The assembly of these nitrogen heterobicycles is a

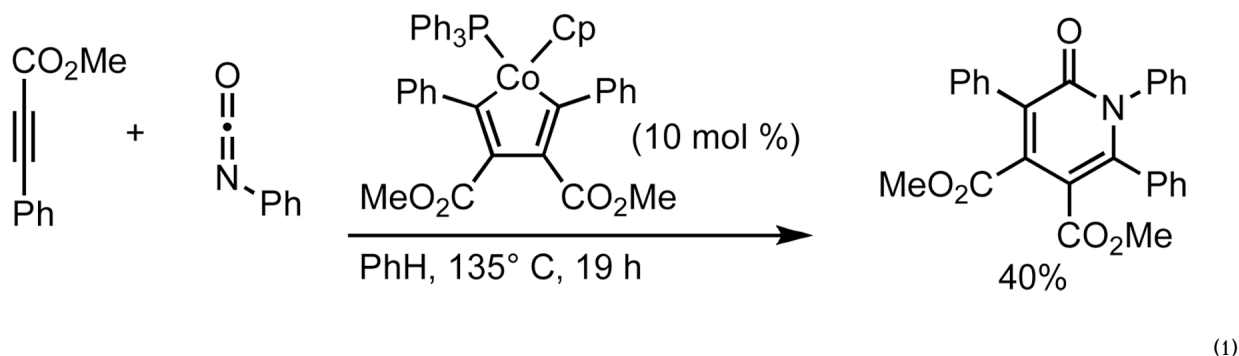
*rovis@lamar.colostate.edu.

Supporting information available. Experimental procedures and spectral data for all new compounds (PDF), as well as cif files for all new crystal structures. This material is available free of charge via the Internet at <http://pubs.acs.org>.

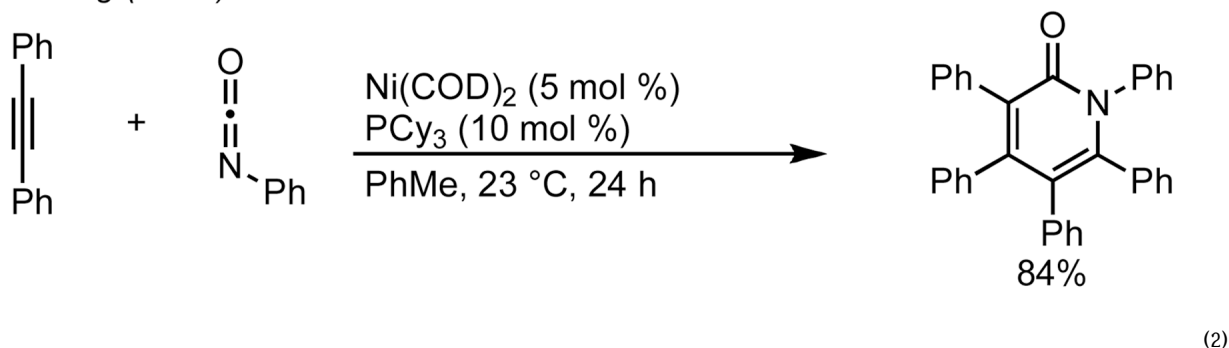
proving ground for synthetic methodology.² Classic syntheses rely on S_N2 cyclization of amines, lactamization, and ring closing metathesis.³ New methodology showcased in the construction of these natural products depend on chiral pool substrates or require lengthy starting material syntheses.^{4,5,6,7,8,9} Therefore, the development of new, rapid, and enantioselective methods to generate nitrogen-containing bicycles would be a useful contribution to the synthetic community.

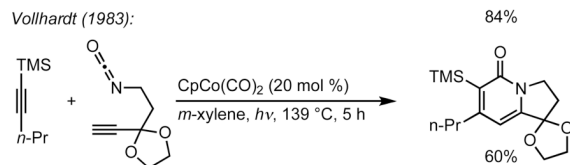
We envisioned the coupling of three separate π -components: $C=N$, $C=C$, and $C\equiv C$ in a metal-catalyzed, [2+2+2] cycloaddition¹⁰ to construct these bicycles (Scheme 1). Due to their modest basicity, isocyanates¹¹ have been shown to be competent partners in transition metal-catalyzed reactions.¹² Yamazaki and Hoberg demonstrated that cobalt and nickel catalyze the [2+2+2] cycloaddition of an isocyanate and two equivalents of an alkyne to form 2-pyridone (eq 1-2).¹³ Vollhardt later found that cobalt can couple an alkynyl isocyanate with an exogenous alkyne to form bicyclic pyridones (eq 3) and applied this methodology to the synthesis of camptothecin.¹⁴ More recently, rhodium, cobalt, nickel, and ruthenium have been shown to catalyze [2+2+2] cycloadditions of alkynes and isocyanates, forming pyridones.¹⁵ Although useful for the synthesis of heterocycles, these methods use two alkynes to form achiral cycloadducts. A notable exception is Tanaka's use of a chiral rhodium complex to access pyridone atropisomers.¹⁶ It would be a clear benefit if an alkene could be incorporated in place of one of the alkynes to form an sp^3 stereocenter in a reaction that could be rendered asymmetric.

Yamazaki (1977):



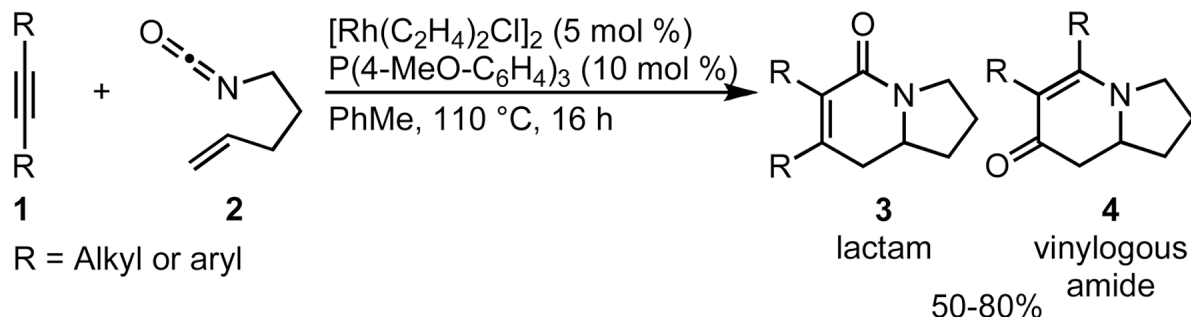
Hoberg (1982):





(3)

Rovis (2006):



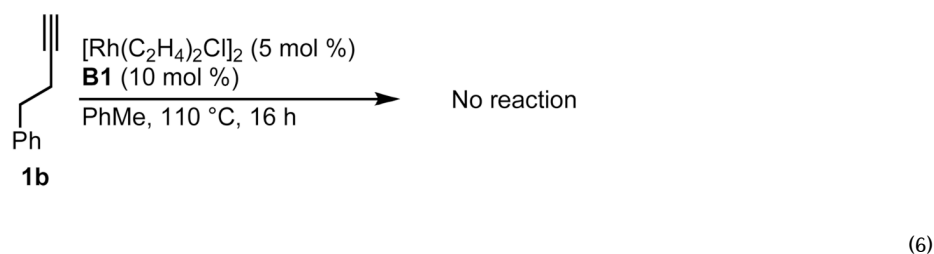
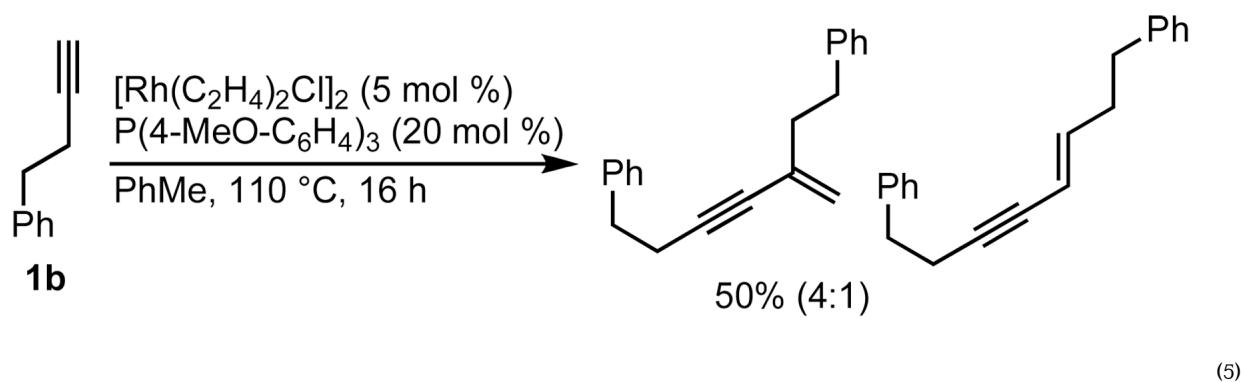
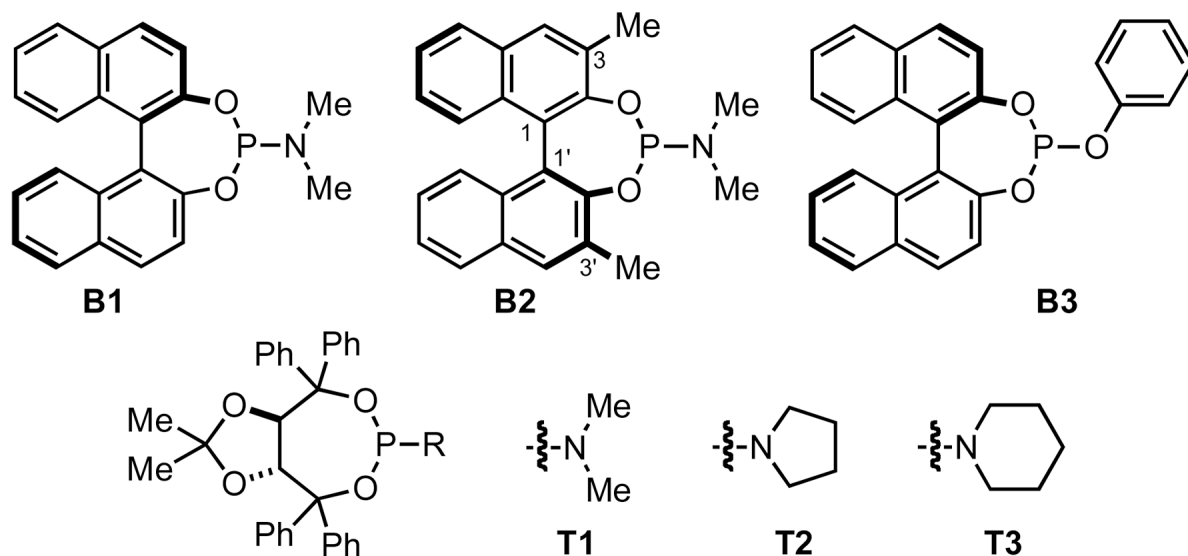
(4)

Prior to our work, three component [2+2+2] cycloadditions between an isocyanate, alkene, and alkyne were unknown.¹⁷ In 2006, we demonstrated that a rhodium(I)/tris(*para*-methoxyphenyl)phosphine complex catalyzes the [2+2+2] cycloaddition of 4-pentenyl isocyanate with symmetrical internal alkynes (eq 4).^{17a} Our initial studies revealed that dialkyl alkynes provide lactam **3** while diaryl alkynes favor vinylogous amide **4**, which arises from fragmentation of the isocyanate moiety (*vide infra*). To increase the utility of the reaction, we expanded the substrate scope to readily available terminal alkynes and rendered the transformation asymmetric with chiral phosphoramidite ligands.^{17b} A variety of structurally and electronically different terminal alkynes and isocyanates are tolerated, enabling the synthesis of a wide range of indolizidines and quinolizidines. Herein, we disclose a full description of the development of this reaction, the effects of steric and electronic changes of the phosphoramidite ligand, single X-ray crystal analysis of six previously unpublished rhodium(cod)chloride/phosphoramidite complexes, and mechanistic insight into the rhodium-catalyzed [2+2+2] cycloaddition of terminal alkynes and alkenyl isocyanates.

Initial ligand screen

Our initial efforts to incorporate terminal alkynes began with an examination of the conditions that were effective for internal alkynes.^{17a} We found that the ligand tris(*para*-methoxyphenyl)phosphine provides less than 20% of **3a** and **4a** in a 1:1 ratio (Table 1, entry 1); the low yield is due to the known dimerization of terminal alkynes (eq 5).¹⁸ BINAP gives no desired product while dppb affords only trace amounts of **3a**, suggesting that a monodentate ligand is required (Table 1, entries 2, 3). MonoPhos (**B1**) affords a 32% yield and induces a modest 55% ee (entry 4). In addition to higher yields, phosphoramidites do not promote dimerization of terminal alkynes (eq 6). Binol-based phosphoramidite **B2** provides a slightly higher yield of vinylogous amide but poor enantioselectivity, while phosphite **B3** shows lower yields than **B1** and **B2** (Table 2, entries 5, 6). Finally, we were delighted to find that Taddol-based phosphoramidite **T1** increases the yield (80%), product selectivity toward vinylogous amide (1:7.0), and

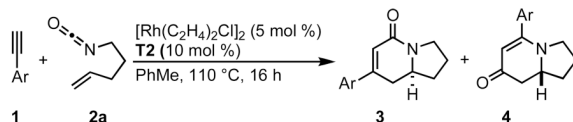
enantioselectivity (94%, entry 7). After modifying the amine, we found **T2** was the optimal ligand for this transformation (entry 8).



Scope of Terminal Alkynes

We investigated the scope of this reaction with terminal aryl alkynes (Table 2) and found electron-rich aryl alkynes provide exclusively vinylogous amide **4** in good yield and high enantioselectivity (entries 1–4).¹⁹ In addition, sterically bulky *o*-substituted aryl alkynes are tolerated (entry 3). Alkynes bearing a variety of heterocycles, including protected and unprotected indoles, readily participate, providing vinylogous amide with high enantioselectivity (entries 5–7). As the alkyne is made more electron-deficient, increasing

amounts of lactam **3** are seen (entries 10–14). Vinylogous amide product formation is not limited to aryl acetylenes; 1-ethynylcyclohexene **1p** gives **4p** exclusively in a 96% yield and 92% ee (entry 15). The reaction clearly shows that substrate electronics can be used to tune product selectivity. A plot of electron-rich and deficient aryl alkynes versus Hammett $\sigma_{m/p}$ values²⁰ indicates a clear linear free energy relationship, demonstrating that the electronics of the alkyne can be used to tune product selectivity (Figure 2). In general, the electronics of the aryl alkyne bias product selectivity such that electron-rich favor vinylogous amide while strongly electron-deficient generate lactam.



Alkyl alkynes shift product selectivity toward the lactam adduct with moderate to good yields (Table 3). An initial ligand screen using Taddols **T1–T3** revealed piperidine-substituted **T3** to be optimal (for a complete comparison, see Table 4). Enantioselectivities with alkyl alkynes and **T3** are moderate (76–87%, entries 1–5, 7, 8). Biphenol based phosphoramidite **A1** leads to an inversion in product selectivity with aliphatic alkynes, preferentially forming vinylogous amide adducts **4** with excellent enantioselectivities (88–94% ee, entries 1–4, 6, 8–13). Esters, amides, and silyl ethers are tolerated with moderate yields and enantioselectivities (entries 2, 5, 6 and 13). Interestingly, bulky cyclohexylacetylene **1w** leads to an increased amount of vinylogous amide with **T1** relative to other aliphatic alkynes (1.2:1), while ligand **A1** generates the vinylogous amide with high product selectivity and excellent ee (14:1, 91% ee, entry 8). Noteworthy is the successful incorporation of 1,7-octadiyne and 1,8-nonadiyne, with ligand **A1** affording vinylogous amides **4y** and **4z** in good yields and high ee's (entries 10–11). On the other hand, 1,6-heptadiyne exclusively furnishes the substituted benzene arising from intramolecular cyclization of the diyne followed by incorporation of a second equivalent of alkyne. These results suggest that, except for the case of a 3-carbon tether linking the diyne, an isocyanate is incorporated in the initial oxidative cycloaddition in preference to an intramolecular coordination and activation of a second terminal alkyne.²¹

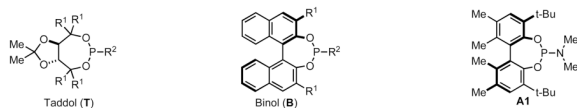
Ligand Exploration

An examination of the structure and electronics of the phosphoramidite revealed that the reaction is sensitive to both (Table 4).²² In general, Taddol-based phosphoramidites (**T1–T9**) give more lactam product with aliphatic alkynes, while Binol and biaryl phosphoramidites (**B1–B6**, **A1**) favor vinylogous amide. Interestingly when the amine of Taddol ligands is changed from pyrrolidine **T2** to piperidine **T3**, product selectivity shifts in favor of lactam **3** from 1:7.3 to 1:3.3 with phenyl acetylene and 2.4:1 to 5:1 with 1-octyne (entries 2, 3), and this trend can be extended to all of the Taddol ligands (entries 1–9). We suspect that it is the size of the amine that is affecting product selectivity, as the basicities of pyrrolidine (11.27 pKa) and piperidine (11.22 pKa) are very similar.²³ Furthermore, very large amines, such as dicyclohexyl amine, completely favor the lactam product, albeit in low yield (entry 4). Interestingly, the size of the amine has less effect on product selectivity with Binol/biaryl phosphoramidites (entries 12–14). These results show that the sterics of the phosphoramidite play a major role in determining product selectivity.

To investigate the effect of ligand electronics, we synthesized a ligand (**T7**) that differs from **T6** only in the aryl substituents: *p*-MeC₆H₄ vs *p*-CF₃C₆H₄ (entry 7). This more electron-deficient ligand increases product selectivity for vinylogous amide with both aryl (1:20 from 1:2.8) and alkyl alkynes (1:1 from 8.3:1), demonstrating that the ligand electronics can enhance

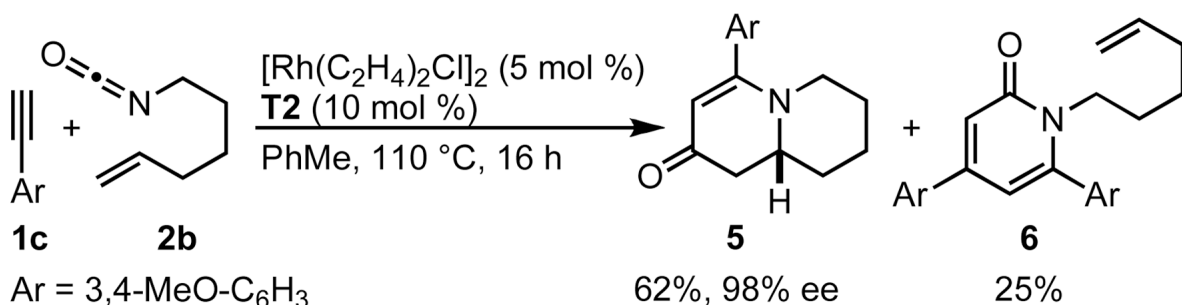
product selectivity. Also, electron-rich *m*-xylyl Taddol **T9** gives a relative increase in the amount of lactam product formed with aryl (1:1.6) and alkyl acetylenes (12.5:1, entry 9).

Taddol ligands provide the best enantioselectivities for aryl alkynes (81–97%, entries 1–9) with **T8** being optimal, while Binol and biaryl ligands give higher enantioselectivity for alkyl alkynes (59–95%, entries 10–14) with **B4** and **B5** being the highest. Substitution at the 3,3'-positions of the Binol/biaryl proves to be essential to improving the enantioselectivity with alkyl acetylenes. Biaryl **A1** provides the highest product ratio (1:6.2) and excellent enantioselectivity (91%) for vinylogous amide with alkyl acetylenes (entry 15). Finally, **A1** made possible the construction of indolizidine (–)-209D²⁴ in a 5-step synthesis from commercially available starting materials, using **4q** as the key intermediate.^{17e}

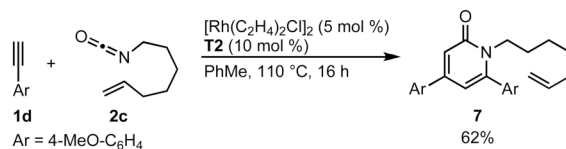


Alkenyl Isocyanate Scope

The successful incorporation of homologous alkenyl isocyanates in this transformation would allow access to quinolizidine natural products. Indeed a longer tether length is tolerated, but in lengthening the tether, we observe a significant amount of 2-pyridone **6** side product (eq 7). A further increase in tether length to heptenyl isocyanate does not provide the desired 1-azabicyclo[5.4.0]undecane, forming only 2-pyridone **7** (eq 8). The synthetic utility of this approach to quinolizidine motifs was demonstrated in the 4-step synthesis of (+)-lasubine II.^{17b}



(7)



(8)

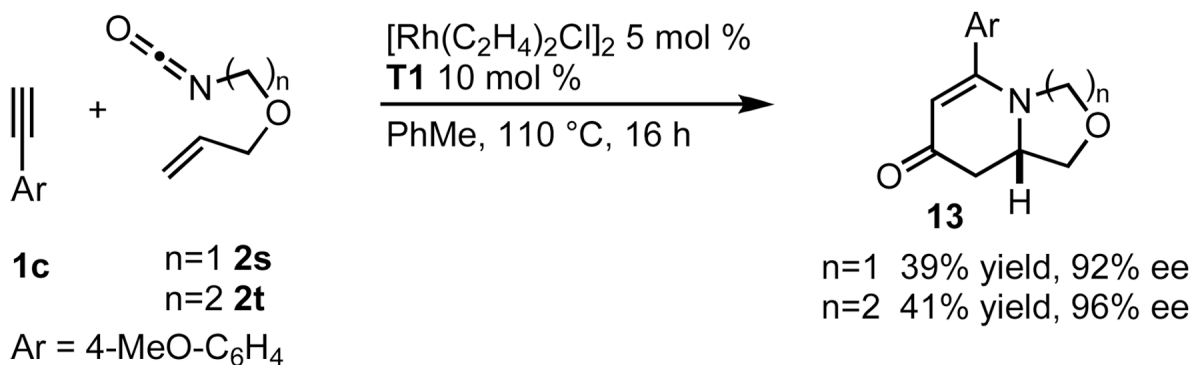
The cycloaddition of 1,1-disubstituted alkenyl isocyanate **2d** with a variety of conjugated aryl and alkenyl alkynes provides indolizinones bearing a tetrasubstituted stereocenter (Table 5). Electron-rich alkyne **1d** gives exclusively vinylogous amide **9d** in 80% yield with 91% ee (entry 1). Heterocyclic and conjugated terminal alkynes react smoothly to afford **9** in good

yields and enantioselectivity (entries 2–6). We see a general trend that as the aryl alkyne becomes more electron-deficient, increasing amounts of the lactam **8** are generated (entry 7). This is consistent with the results seen with 4-pentenyl isocyanate **2a** (*vide supra*).

Alkyl alkynes and 1,1-disubstituted alkenyl isocyanates provide mostly lactam **8** with enantioselectivities ranging from 91% to 95% ee (Table 6). Functional groups including protected alcohols, halogens, and internal alkynes are tolerated (entries 5–8). Silyl alkynes fail to participate in this reaction; this finding allowed the chemoselective incorporation of mono-protected 1,6-diynes (entry 8).

Variations of the 1,1-disubstituted alkene furnish tetrasubstituted indolizinones with a range of substitution at the 9 position (Table 7). Substrates bearing primary alkyl groups on the olefin react smoothly with high enantioselectivity (entries 1–5). However, the reaction is sluggish with secondary alkyl substituents and increasing amounts of pyridone are seen (entries 6, 7). Protected alcohols, halogens, and alkenes are tolerated in the reaction, providing handles for further chemical manipulation (entries 9–11).

Substitution on the alkenyl isocyanate tether is tolerated in the cycloaddition (Table 8). Diethyl malonate derived alkenyl isocyanate **2p** provides yields and enantioselectivities comparable to **2a** (entries 1, 2). Geminal dimethyl substituents on the tether react smoothly providing good yields and selectivities with **T1** (entries 3, 4). This backbone substitution is also tolerated with 1,1-disubstituted alkenes, affording optimal selectivities when ligand **A1** is used (entry 6). Oxygen substitution in the tether provides **13** in moderate yields and excellent enantioselectivities up to 96% ee (eq 9).



(9)

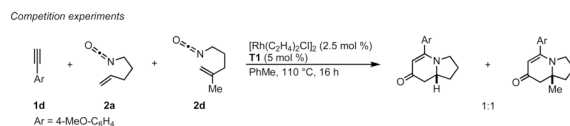
Mechanistic Investigation

The proposed catalytic cycle for the [2+2+2] cycloaddition of alkenyl isocyanates with exogenous alkynes to form lactam, vinylogous amide, 2-pyridone, and 4-pyridone products is described in Scheme 2. All products may be accessed from a common coordination of the alkyne and isocyanate to form the Rh(I)/phosphoramidite complex (**I**). From this complex, oxidative cyclization and C–C bond formation provides **IIa**.²⁵ Migratory alkene insertion into **IIa** generates seven-membered rhodacycle **IIIa**, which reductively eliminates to generate lactam **3**. Alternatively, the rhodium(I) coordination complex (**I**) can oxidatively cyclize to form **IIb**, where C–N bond formation occurs first. However, the alkene is unable to insert into the resultant rhodium(III) species **IIb** presumably due to a strained, bridged geometry in the transition state. A CO migration via **IIb** then takes place to form **IVb**.²⁶ At this point, migratory alkene insertion gives rhodacycle **Vb**, and reductive elimination provides vinylogous

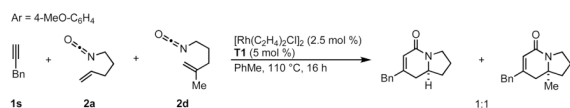
amide **4**. Additionally, formation of 2-pyridone can be generated from an exogenous alkyne intercepting either **IIa** or **IIb**.^{17c} 4-pyridone can be formed from alkyne interception of rhodacycle **IVb**, and its isolation from a similar catalytic system is further evidence for the formation of **IVb**.²⁷

Another catalytic cycle can be imagined in which the alkene of the alkenyl isocyanate coordinates to the rhodium (**VI**) in lieu of an alkyne (Scheme 3). Such coordination would lead to oxidative cyclization, C–N bond formation, and set the stereochemistry for both lactam and vinylogous amide products in the formation of the bicyclic rhodacycle **VII**. Migratory alkyne insertion would give **IIIa** and subsequent reductive elimination would generate lactam **3**. Alternatively, a CO migration via **VIII** could take place prior to alkyne insertion making bicycle **IX**, which would then undergo alkyne insertion (**X**) and reductive elimination to form vinylogous amide **4**.

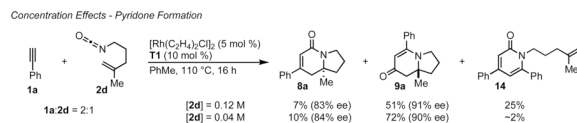
Several observations suggest that this alternative mechanism is not the operative catalytic cycle. First, two competition experiments were conducted between mono (**2a**) and 1,1-disubstituted (**2d**) alkenyl isocyanates (eqs 10, 11) in the presence of either aryl (**1d**) or alkyl (**1s**) acetylenes. These yield a 1:1 ratio of vinylogous amide or lactam products respectively. We would predict that isocyanate **2a** should react at a different rate than **2d** leading to an unequal product mixture.²⁸ Because olefin substitution has no effect on the ratio of products obtained, we propose that the olefin is not involved in the turnover-limiting step. Second, higher reaction concentrations (0.12 M vs 0.04 M) (eq 12) or bulky alkene substituents increase pyridone formation.²⁹ Higher concentrations favor intermolecular interception of metallacycle **IIa/b** by a second equivalent of alkyne over intramolecular migratory insertion of the tethered alkene. Furthermore, bulky substituents inhibit migratory insertion of the alkene favoring intermolecular insertion of a second alkyne to form pyridone. These results suggest that the alkyne and isocyanate are the first components to oxidatively cyclize. This is further supported by the observation that 1,7-octadiyne **1y** and 1,8-nonadiyne **1z** furnish vinylogous amides **4y** and **4z** showing an apparent kinetic preference for *intermolecular* coordination and activation of the isocyanate in spite of the entropically favored *intramolecular* coordination of the second terminal alkyne (Table 3, entries 10, 11). While individually the preceding pieces of evidence do not eliminate the alternate catalytic cycle shown in Scheme 3, their aggregate suggests them to be unlikely. Finally, the vinylogous amide and lactam products obtained with the same Taddol phosphoramidite are opposite major enantiomers. This suggests that both products are not formed from rhodacycle **VII** as stereoinduction would occur prior to CO migration. Considering these observations, we propose that the alkene is the last π -component to be incorporated and the operative catalytic cycle is likely that shown in Scheme 2.³⁰



(10)



(11)



(12)

We see remarkable regioselectivity in this rhodium-catalyzed cycloaddition, where the vinyl hydrogen is α to the carbonyl in all terminal alkyne products. As part of our ongoing efforts to explain the regio- and product selectivity of the reaction, single crystal X-ray analyses³¹ of rhodium(I)(cod)chloride/phosphoramidite complexes³² were undertaken. In each of these structures, rhodium is in a square planar geometry and a strong phosphoramidite *trans* influence is displayed. Generally, Taddol-based phosphoramidites have a weaker *trans* influence than Binol/biaryl phosphoramidite as seen by the Rh–alkene distance (Table 9).

After examining the X-ray crystal structures, we hypothesize that the steric environment created by monodentate, C_2 -symmetric phosphoramidite ligands explains the exceptional regioselectivity in the cycloaddition. As we have depicted in Figure 3, the phosphoramidite ligands sterically hinder one face of the square planar rhodium(I) complex. One of the *m*-xylyl groups sits above the Rh square plane in the structure of **T8**•Rh(cod)Cl, with the opposite side of the complex much more exposed. A naphthyl ring plays this role in the **B4**•Rh(cod)Cl complex, reinforced by the TMS group. These effects are also evident in other Rh•phosphoramidite crystal structures.³² We propose that this hindrance biases the coordination of the alkyne and isocyanate such that the sterically smaller substituents are in the same hemisphere of the square plane as shown in **I** (Fig 2). We suggest that the alkynes displace the ethylene prior to the association of the isocyanate, and as the phosphoramidite has the greater *trans* influence than chloride, we predict that the isocyanate coordinates *trans* to the phosphoramidite. From this single coordination, oxidative cyclization accounts for the single regioisomer of the lactam and vinylogous amide. Thus, we propose that regioselectivity is controlled predominately by the sterics of the phosphoramidite ligand.

It may be argued that the alkyne and isocyanate coordinate to the metal parallel to the square plane.³³ However, Wakatsuki and Yamazaki's calculations of cobaltacyclopentadienes³⁴ and ground state X-ray crystal analysis of other d^8 complexes³⁵ suggest that an orthogonal coordination of π -components is operative because steric repulsion between π -components is minimized and better back donative stabilization is possible when orthogonal. Wakatsuki-Yamazaki's regioselectivity model is based on observations and calculations of cobaltacyclopentadiene formation (Scheme 4). The major product results from a head to tail orientation of the large alkyne substituents to form cobaltacyclopentadiene **14**. We do not observe either lactam or vinylogous amide products derived from such an orientation. Wakatsuki and Yamazaki claim the minor product **15** is kinetically favored over **16** due to steric interactions between large alkyne substituents as shown in **TSIII** (Scheme 4). When the alkynes are not head to tail, they suggest that the large substituents prefer to be α to the metal. This model accounts for the regioselectivity seen with rhodacycle **IIa**, which generates lactam (Scheme 2). Using this argument, one would predict that larger alkyne substituents would favor lactam; however, more vinylogous amide is seen (Table 3, entry 1 vs 8). Finally, this model does not account for vinylogous amide formation, since the larger groups are β to the metal in rhodacycle **IIb** (Scheme 2). As product selectivity could not be completely explained by substrate steric control alone, we sought another model to rationalize selectivity based on stereoelectronic effects.

Stockis and Hoffman in their theoretical treatise on metallacyclopentane formation discuss the effects that polarized π components have on regioselectivity in the absence of steric

contributions.³⁶ As a result of their calculations and subsequent correlation with experimental data, they propose a model based on stereoelectronic effects to explain regioselectivity. They hypothesize that polarized π components oxidatively cyclize so that the greatest LUMO coefficient is β to the metal, due to enhanced π^* mixing with filled d_{xy} orbitals in the transition state (Scheme 4). In our system, we observe a propensity for lactam formation when the sterics of the phosphoramidite and alkyne substrate decrease. Presumably, this is due to the large LUMO coefficient of the isocyanate at the β position, lowering the activation energy for **TSIV** en route to metallacycle **IIa** (Scheme 5). However, it does not explain the regioselectivity of the isocyanate in **TSV** for vinylogous amide formation or lactam products derived from electron-rich aryl acetylenes or alkyl acetylenes. In each of the cases discussed, the largest LUMO of one of the π -components is α to the metal in the resultant metallacycle contrary to Stockis-Hoffman.

As neither the Wakatsuki-Yamazaki steric nor the Stockis-Hoffman stereoelectronic model adequately explain the product selectivity seen in the cycloaddition, we hypothesize that the reaction is controlled primarily by sterics and enhanced or diminished by electronic factors (Scheme 5). Single regioisomeric products are explained by alkyne and isocyanate coordination dictated by phosphoramidite sterics, placing the small substituent of each π -component in a *cis* orientation. The two π -components are coordinated orthogonal to the square plane, as proposed by Wakatsuki-Yamazaki and corroborated by crystal structures.³⁷ To generate rhodacycle **IIa** en route to lactam from the orthogonal coordination seen in **Ia**, the CO of the isocyanate and the terminal C–H of the alkyne must bend away from the Rh center and toward each other passing through **TSIV** forming the C–C bond. Similarly, the N–R² group of the isocyanate and the C–R¹ bond of the terminal alkyne bend away from the Rh center, forming the C–N bond via **TSV**, en route to rhodacycle **IIb** in the vinylogous amide pathway.

In terms of product selectivity, the LUMO of the isocyanate favors formation of lactam, but is overridden by sterics of the substrate and ligand. Smaller alkynes (1-octyne, Table 3, entry 1) generate lactam, while larger alkynes (cyclohexylacetylene, Table 3, entry 7) produce vinylogous amide due to ligand-alkyne interactions in the transition state (Scheme 5, **TSIV**). Alkyne electronics modify product selectivity as seen in Figure 2. Electron-deficient aryl alkynes override steric control to favor lactam, as the alkyne and isocyanate LUMOs are β to the metal in **TSIVb**. Electron-rich aryl alkynes generate vinylogous amide due to unfavorable steric interactions between the alkyne and ligand (**TSIV**), and this selectivity is reinforced by the alkyne LUMO because it is β to the metal in **TSVa**.

These unfavorable alkyne-phosphoramidite interactions are augmented by changes in the Rh–P bond length, where a shorter bond favors vinylogous amide while a longer bond favors lactam (Table 9). Electron-deficient phosphoramidites have shorter Rh–P bond lengths, which exacerbate the ligand alkyne interaction in the transition state leading to more vinylogous amide. On the other hand, electron-rich phosphoramidites have longer Rh–P bonds, which alleviate the steric interactions between the alkyne and ligand to generate more lactam. Additionally, we have seen that in the Taddol series large amines favor lactam product presumably by increasing the Rh–P bond length.

Stereochemical Model

A proposed model that rationalizes the observed enantioselectivity is depicted in Scheme 6. In metallacycle **IIa** leading to lactam, we postulate that there are two factors controlling enantioinduction: facial selectivity of the alkene dictated by the geometry of the tether and facial selectivity at rhodium as influenced by the phosphoramidite ligand. Each of the rhodium (cod)chloride•phosphoramidite crystal structures show that the ligand hinders one of the open faces on rhodium and we suggest this facial hindrance is present in the rhodium(III)

intermediates. For migratory insertion to occur the alkene must be *syn*-coplanar with the Rh—N bond, and as a result, only four alkene coordination scenarios can be envisioned. In the first two scenarios, **IIa^A** and **IIa^B**, the alkene has to coordinate to the hindered rhodium face, which is disfavored. Additionally, **IIa^A** requires the alkene tether to be in an undesirable twist-boat conformation further disfavoring it; in **IIa^B** the tether can adopt a chair conformation and 1,2-migratory insertion leads to the minor enantiomer. In the second two scenarios, **IIa^C** and **IIa^D**, we propose that the alkene coordinates to the less hindered face of rhodium. Alkene coordination is disfavored in **IIa^C** because the tether would be in a strained twist-boat conformation. On the other hand, the tether shown in metallacycle **IIa^D** is in a favorable chair conformation and migratory insertion provides the major lactam enantiomer. This model for lactam enantioselectivity rationalizes the correct absolute stereochemistry observed; however, it assumes no rearrangement of the unobservable rhodium(III) intermediates.

Rationalizing enantioselectivity for vinylogous amide is more difficult because enantioinduction presumably occurs after several ligand rearrangements on rhodium(III) species. CO migration from **IIIb** probably occurs from amide bond cleavage and amine migration to the unhindered open coordination site, resulting in metallacycle **IIIb^{A,B}**. We speculate that the alkenyl carbon migrates to the CO ligand as seen in **IIIb^A** leading to metallacycle **IVb^A**. However, coordination of the alkene and migratory insertion of this metallacycle leads to the minor enantiomer observed for vinylogous amide. The major enantiomer could be formed by CO migration onto the alkenyl carbon (**IIIb^B**), but such a migration is unprecedented.²⁶ Rapid rearrangement of **IVb^A** to **IVb^B** and subsequent alkene insertion would provide the major observed enantiomer. This rearrangement is potentially influenced by steric interactions between the alkenyl tether and ligand disfavoring **IVb^A**.³⁸ As these models are for an unobservable rhodium(III) species, we can only speculate as to the actual ligand rearrangements. These models are tentative and we are currently undertaking computational studies to rationalize enantioinduction.

Conclusion

In conclusion, we have developed a rapid, efficient, and highly enantioselective cycloaddition of alkenyl isocyanates and exogenous alkynes to access indolizidine and quinolizidine cores found in biologically relevant natural products. We have found that single regioisomeric products are obtained in good yields and excellent enantioselectivities. X-ray crystal analysis of rhodium(cod)chloride/phosphoramidite complexes has led us to a mechanistic hypothesis that accounts for the single regioisomeric products obtained. In conjunction with competition experiments and pyridone formation, we have suggested a catalytic cycle that accounts for both the lactam and vinylogous amide products. We conclude that the regio- and product selectivity are controlled primarily by the sterics of the phosphoramidite ligand and substrate, while the electronics of both either enhance or diminish product selectivity.

Supplementary Material

Refer to Web version on PubMed Central for supplementary material.

Acknowledgments

We thank NIGMS (GM80442) for support. DMD thanks NSF-LSAMP Bridge to the Doctorate Program for support. SP thanks the FQRNT for a postdoctoral fellowship. RTY thanks Lilly for a graduate fellowship. KMO and DMD thank Oren Anderson and Susie Miller (CSU) for support and guidance. TR thanks the Monfort Family Foundation for a Monfort Professorship. We thank Johnson Matthey for a loan of rhodium salts.

References

1. (a) Daly JW. *J. Med. Chem* 2003;46:445–452. [PubMed: 12570366] (b) Daly JW, Spande TF, Garraffo HM. *J. Nat. Prod* 2005;68:1556–1575. [PubMed: 16252926]
2. For reviews of recent syntheses, see: (a) Michael JP. *Nat. Prod. Rep* 2000;17:579–602. [PubMed: 11152422] (b) Michael JP. *Nat. Prod. Rep* 2002;20:458–475. [PubMed: 14620842] (c) Michael JP. *Nat. Prod. Rep* 2005;22:603–626. [PubMed: 16193159] (d) Michael JP. *Nat. Prod. Rep* 2007;24:191–222. [PubMed: 17268613] (e) Michael JP. *Nat. Prod. Rep* 2008;25:139–165. [PubMed: 18250900]
3. For selected syntheses: (a) Kim G, Jung S-d, Kim W-j. *Org. Lett* 2001;3:2985–2987. [PubMed: 11554824] (b) Toyooka N, Fukutome A, Nemoto H, Daly JW, Spande TF, Garraffo HM, Kaneko T. *Org. Lett* 2002;4:1715–1717. [PubMed: 12000281] (c) Hermet J-PR, McGrath MJ, O'Brien P, Porter DW, Gilday J. *Chem. Commun* 2004:1830–1831. (d) Zaja M, Blechert S. *Tetrahedron* 2004;60:9629–9634. (e) Toyooka N, Kawasaki M, Nemoto H, Awale S, Tezuka Y, Kadota S. *Synlett* 2005:3109–3110. (f) Toyooka N, Dejun Z, Nemoto H, Garraffo HM, Spande TF, Daly JW. *Tetrahedron Lett* 2006;47:577–580.
4. For tandem conjugate additions, see: (a) Back TG, Nakajima K. *J. Org. Chem* 1998;63:6566–6571. (b) Ma D, Zhu W. *Org. Lett* 2001;3:3927–3929. [PubMed: 11720571] (c) Back TG, Hamilton MD, Lim VJJ, Parvez M. *J. Org. Chem* 2005;70:967–972. [PubMed: 15675856] (d) Cai G, Zhu W, Ma D. *Tetrahedron* 2006;62:5697–5708.
5. For cascade reactions, see: (a) Amorde SM, Judd AS, Martin SF. *Org. Lett* 2005;7:2031–2033. [PubMed: 15876047] (b) Padwa A, Bur SK. *Tetrahedron* 2007;63:5341–5378. [PubMed: 17940591]
6. For the use of dihydro-4-pyridones as synthons, see: (a) Joseph S, Comins DL. *Curr. Opin. Drug Discovery Dev* 2002;5:870. (b) Young DW, Comins DL. *Org. Lett* 2005;7:5661–5664. [PubMed: 16321016]
7. For intramolecular Schmidt reaction, see: (a) Aubé J, Milligan GL. *J. Am. Chem. Soc* 1991;113:8965–8966. (b) Gracis V, Zeng Y, Desai P, Aubé J. *Org. Lett* 2003;5:4999–5001. [PubMed: 14682749]
8. For a three component coupling using silyl dithianes, see: (a) Smith AB III, Kim D-S. *Org. Lett* 2004;6:1493–1495. [PubMed: 15101775] (b) Smith AB III, Kim D-S. *J. Org. Chem* 2006;71:2547–2557. [PubMed: 16555804]
9. For a catalytic, asymmetric aza-Diels-Alder reaction, see: (a) García-Mancheño O, Gómez-Arrayás R, Carretero JC. *J. Am. Chem. Soc* 2004;126:456–457. [PubMed: 14719929] (b) García-Mancheño O, Gómez-Arrayás R, Adrio J, Carretero JC. *J. Org. Chem* 2007;72:10294–10297. [PubMed: 18027970]
10. For reviews on [2+2+2] cycloadditions of alkynes see: (a) Saito S, Yamamoto Y. *Chem. Rev* 2000;100:2901–2915. [PubMed: 11749309] (b) Agenet N, Busine O, Slowinski F, Gandon V, Aubert C, Malacria M. *Org. React* 2007;68:1–302. (c) Galan BR, Rovis T. *Angew. Chem. Int. Ed* 2009;48:2830–2834. For reviews on [2+2+2] cycloadditions of alkynes and nitrogen moieties see: (d) Varela JA, Saá C. *Chem. Rev* 2003;103:3787–3801. [PubMed: 12964884] (e) Heller B, Hapke M. *Chem. Soc. Rev* 2007;36:1085–1094. [PubMed: 17576476] (f) Chopade PR, Louie J. *Adv. Synth. Catal* 2006;348:2307–2327.
11. Ozaki S. *Chem. Rev* 1972;72:457–496.
12. Braunstein P, Nobel D. *Chem. Rev* 1989;89:1927–1945.
13. (a) Hong P, Yamazaki H. *Synthesis* 1977;1:50–52. (b) Hong H, Yamazaki H. *Tetrahedron Lett* 1977;15:1333–1336. (c) Hoberg H, Oster BW. *Synthesis* 1982:324–325. (d) Hoberg H, Oster BW. *J. Organomet. Chem* 1983;234:C35–C38. (e) Hoberg H, Oster BW. *J. Organomet. Chem* 1983;252:359–364.
14. (a) Earl RA, Vollhardt KPC. *J. Am. Chem. Soc* 1983;105:6991–6993. (b) Earl RA, Vollhardt KPC. *J. Org. Chem* 1984;49:4786–4800.
15. Cobalt: (a) Diversi P, Ingrosso G, Lucherini A, Malquori S. *J. Mol. Catal* 1987;40:267–280. (b) Bonaga LVR, Zhang H-C, Moretto AF, Ye H, Gauthier DA, Li J, Leo GC, Maryanoff BE. *J. Am. Chem. Soc* 2005;127:3473–3485. [PubMed: 15755167] Nickel: (c) Takahashi T, Tsai F, Li Y, Wang H, Kondo Y, Yamanaka M, Nakajima K, Kotora M. *J. Am. Chem. Soc* 2002;124:5059–5067. [PubMed: 11982370] (d) Duong HA, Cross MJ, Louie J. *J. Am. Chem. Soc* 2004;126:11438–11439. [PubMed: 15366880] (e) Duong HA, Louie J. *J. Organomet. Chem* 2005;690:5098–5104. (f) Duong HA, Louie J. *Tetrahedron* 2006;62:7552–7559. Ruthenium: (g) Yamamoto Y, Takagishi H, Itoh K. *Org. Lett* 2001;3:2117–2119. [PubMed: 11418063] (h) Yamamoto Y, Kinpara K, Saigoku T,

- Takagishi H, Okuda S, Nishiyama H, Itoh K. *J. Am. Chem. Soc* 2005;127:605–613. [PubMed: 15643884] Rhodium: (i) Flynn ST, Hasso-Henderson SE, Parkins AW. *J. Mol. Catal* 1985;32:101–105. (k) Kondo T, Nomura M, Ura Y, Wada K, Mitsudo T. *Tetrahedron Lett* 2006;47:7107–7111.
16. (a) Tanaka K, Wada A, Noguchi K. *Org. Lett* 2005;7:4737–4739. [PubMed: 16209523] (b) Tanaka K. *Synlett* 2007:1977–1993. (c) Tanaka K, Takahashi Y, Suda T, Hirano M. *Synlett* 2008:1724–1728.
17. (a) Yu RT, Rovis T. *J. Am. Chem. Soc* 2006;128:2782–2783. [PubMed: 16506740] (b) Yu RT, Rovis T. *J. Am. Chem. Soc* 2006;128:12370–12371. [PubMed: 16984159] (c) Lee EE, Rovis T. *Org. Lett* 2008;10(6):1231–1234. [PubMed: 18284249] (d) Yu RT, Rovis T. *J. Am. Chem. Soc* 2008;130:3262–3263. [PubMed: 18302377] (e) Yu RT, Lee EE, Malik G, Rovis T. *Angew. Chem. Int. Ed* 2009;48:2379–2382. (f) Keller Friedman R, Rovis T. *J. Am. Chem. Soc* 2009;131:10775–10782. [PubMed: 19569692]
18. (a) Albano P, Aresta M. *J. Organomet. Chem* 1980;190:243–246. (b) Schäfer H, Marcy R, Rüping T, Singer H. *J. Organomet. Chem* 1982;240:17–25. (c) Ohshita J, Furumori K, Matsuguchi A, Ishikawa M. *J. Org. Chem* 1990;55:3277–3280.
19. In our experience, this chemistry has proven to be very robust. Roughly 25% of all reactions described herein have been conducted multiple times often by different coworkers. We have found that yields vary slightly between runs (~5%) while product selectivities (± 0.2 , e.g. 7.0:1 to 7.2:1) and enantioselectivities ($\pm 0.5\%$) change little. Product selectivity is determined by analysis of ^1H NMR spectra of unpurified reaction mixtures, and can be complicated by unreacted starting material and symmetrical ureas arising from partial hydrolysis of the isocyanate.
20. Hansch C, Leo A, Taft RW. *Chem. Rev* 1991;91:165.
21. TMS-acetylene does not participate under these reaction conditions.
22. During this study, we found that catalyst loading could be reduced from 10 mol % to 5 mol % without sacrificing yield or enantioselectivity.
23. Hall HK. *J. Am. Chem. Soc* 1957;79:5441.
24. (–) Indolizidine-209D is a non-natural indolizidine derived from the misassignment of pyrrolizidine 209-K; see ref 1b.
25. For selected publications with similar metallacycles involving an isocyanate and alkyne see: (a) Hoberg H. *J. Organomet. Chem* 1988;358(1–3):507–517. (b) Duong HA, Louie J. *J. Organomet. Chem* 2005;690(23):5098–5104. (c) Louie J. *Curr. Org. Chem* 2005;9(7):605–623. (d) Yamamoto Y, Kinpara K, Saigoku T, Takagishi H, Okuda S, Nishiyama H, Itoh K. *J. Am. Chem. Soc* 2005;127:605–613. [PubMed: 15643884] (e) Kondo T, Nomura M, Ura Y, Wada K, Mitsudo T. *Tetrahedron Lett* 2006;47(39):7107–7111. (f) Duong HA, Louie J. *Tetrahedron* 2006;62(32):7552–7559. (g) Kondo T, Nomura M, Ura Y, Wada K, Mitsudo T-a. *J. Am. Chem. Soc* 2006;128:14816–14817. [PubMed: 17105286]
26. For selected CO migration references on rhodium(III) species see: (a) Cavallo L, Sola M. *J. Am. Chem. Soc* 2001;123:12294–12302. [PubMed: 11734030] (b) Gonsalvi L, Adams H, Sunley GJ, Ditzel E, Haynes A. *J. Am. Chem. Soc* 2002;124:13597–13612. [PubMed: 12418915] (c) Gonsalvi L. *Organometallics* 2003;22(5):1047–1054.
27. Oberg KM, Lee EE, Rovis T. *Tetrahedron* 2009;65:5056–5061.
28. For a study of the effect of olefin substitution on the thermodynamics of alkene-nickel coordination, see: Tolman CA. *J. Am. Chem. Soc* 1974;96:2780–2789.
29. If pyridone were to be formed by oxidative cycloaddition of two equivalents of alkyne prior to isocyanate incorporation, a different regioisomer would be predicted. Additionally, different alkynes should give different regioisomers as seen by multiple authors (see references ¹⁵ and ¹⁶). Using Rh(I)•A1, we have noted the formation of pyridones as single regioisomers when the reaction is conducted using isocyanates lacking the tethered alkene; see reference ²⁷.
30. A mechanism where the alkyne and alkene oxidatively cyclize to make a rhodacyclopentene followed by isocyanate insertion can be proposed, but this is unlikely because there is no plausible pathway to vinylogous amide and 4-pyridone. For computations proposing alkyne-alkyne cyclization followed by C=N insertion, see: (a) Schmid R, Kirchner K. *J. Org. Chem* 2003;68:8339–8344. [PubMed: 14575455] (b) Dazinger G, Schmid R, Kirchner K. *New J. Chem* 2004;28:153–155. (c) Dazinger G, Torres-Rodrigues M, Kirchner K, Calhorda MJ, Costa PJ. *J. Organomet. Chem* 2006;691:4434–4445.

31. For complete details of the rhodium/phosphoramidite X-ray crystal analysis, see the supplementary information.
32. For publications of rhodium and iridium phosphoramidite crystal structures see: (a) Bartels B, García-Yebra C, Rominger F, Helmchen G. *Eur. J. Inorg. Chem* 2002;2569–2586. (b) Leitner A, Shekhar S, Pouy MJ, Hartwig JF. *J. Am. Chem. Soc* 2005;127:15506–15514. [PubMed: 16262414] (c) Faller JW, Milheiro SC, Parr J. J. *Organomet. Chem* 2006;691:4945–4955. (d) Giacomina F, Meetsma A, Panella L, Lefort L, de Vries AHM, de Vries JG. *Angew. Chem. Int. Ed* 2007;46:1497–1500. (e) Mikhel IS, Ruegger H, Butti P, Camponovo F, Huber D, Mezzetti A. *Organometallics* 2008;27:2937–2948. (f) Filipuzzi S, Maennel E, Pregosin PS, Albinati A, Rizzato S, Veiros LF. *Organometallics* 2008;27:4580–4588.
33. Imabayashi T, Fujiwara Y, Nakao Y, Sato H, Sakaki S. *Organometallics* 2005;24:2129–2140.
34. Wakatsuki Y, Nomura O, Kitaura K, Morokuma K, Yamazaki H. *J. Am. Chem. Soc* 1983;105(7):1907–1912.
35. For crystal structures, see:(a) Davies GR, Hewerston WH, Maise RHB, Owston PG, Patel CG. *J. Chem. Soc* 1970:1873. (b) Beauchamp AL, Rochon FR, Theophanides T. *Can. J. Chem* 1973;51:126. For computational analysis of alkyne coordination to Pd, see: (c) de Vaal P, Dedieu A. *J. Organomet. Chem* 1994;478:121–1129.
36. Stockis A, Hoffmann R. *J. Am. Chem. Soc* 1980;102:2952–2962.
37. Kemmitt and coworkers report the crystal structures of $\text{Rh}(\text{acac})(\text{C}_2\text{H}_4)(\text{CF}_3\text{CCCF}_3)$ and the cyclooctene analog. Both structures show coordination of the olefin and alkyne orthogonal to the square plane. Intriguingly, both complexes show unsymmetrical coordination of the two p-components, with the a atoms having shorter Rh–C distances than the b atoms, even with a ligand as sterically undemanding as acac; see:(a) Barlow JH, Clark GR, Curl MG, Howden ME, Kemmitt RDW, Russell DR. *J. Organomet. Chem* 1978;144:C47–C51. (b) Barlow JH, Curl MG, Russell DR, Clark GR. *J. Organomet. Chem* 1982;235:231–241.
38. It is also possible that the trans influence of the phosphoramidite and chloride dictate the relative stability of **IVb^A** and **IVb^B** (or the corresponding transition states). For a review on computational approaches to studying olefin insertion into metal hydrides, see: Niu S, Hall MB. *Chem. Rev* 2000;100:363–405. and references therein

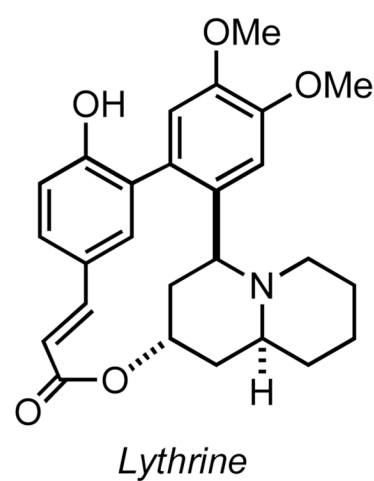
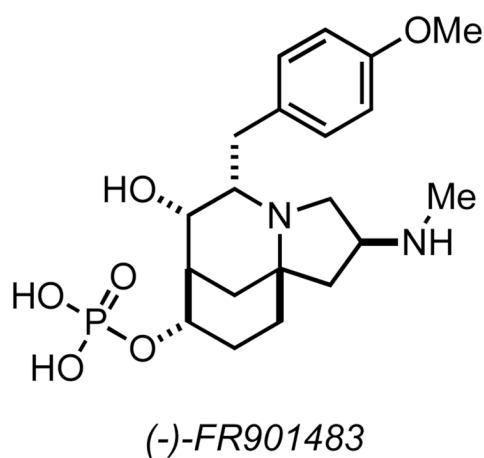
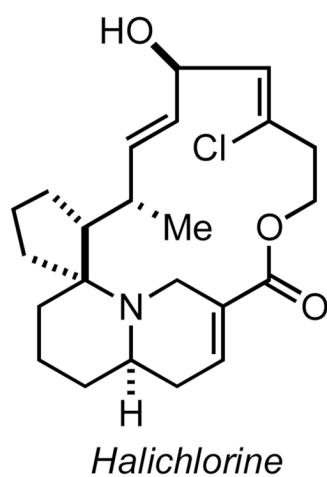
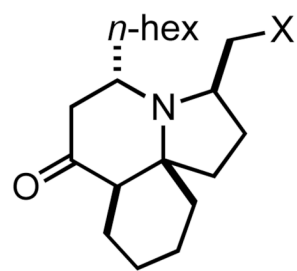
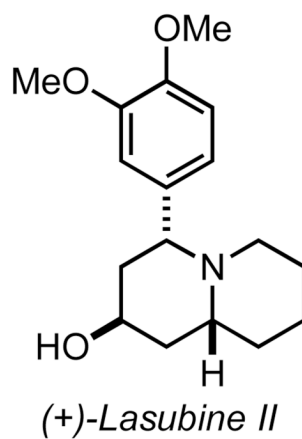
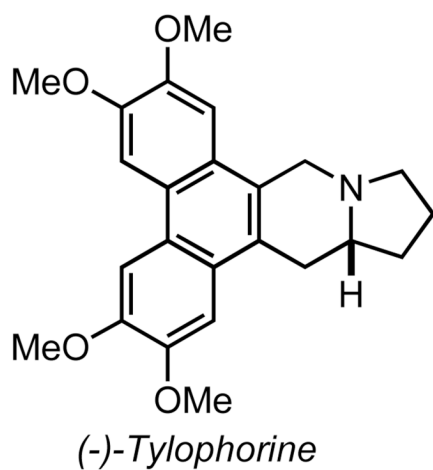
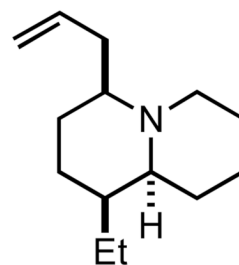
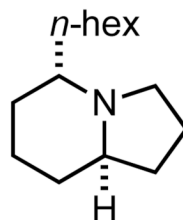
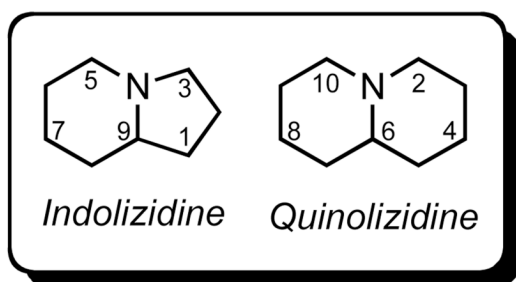


Figure 1.
Indolizidine and quinolizidine natural products.

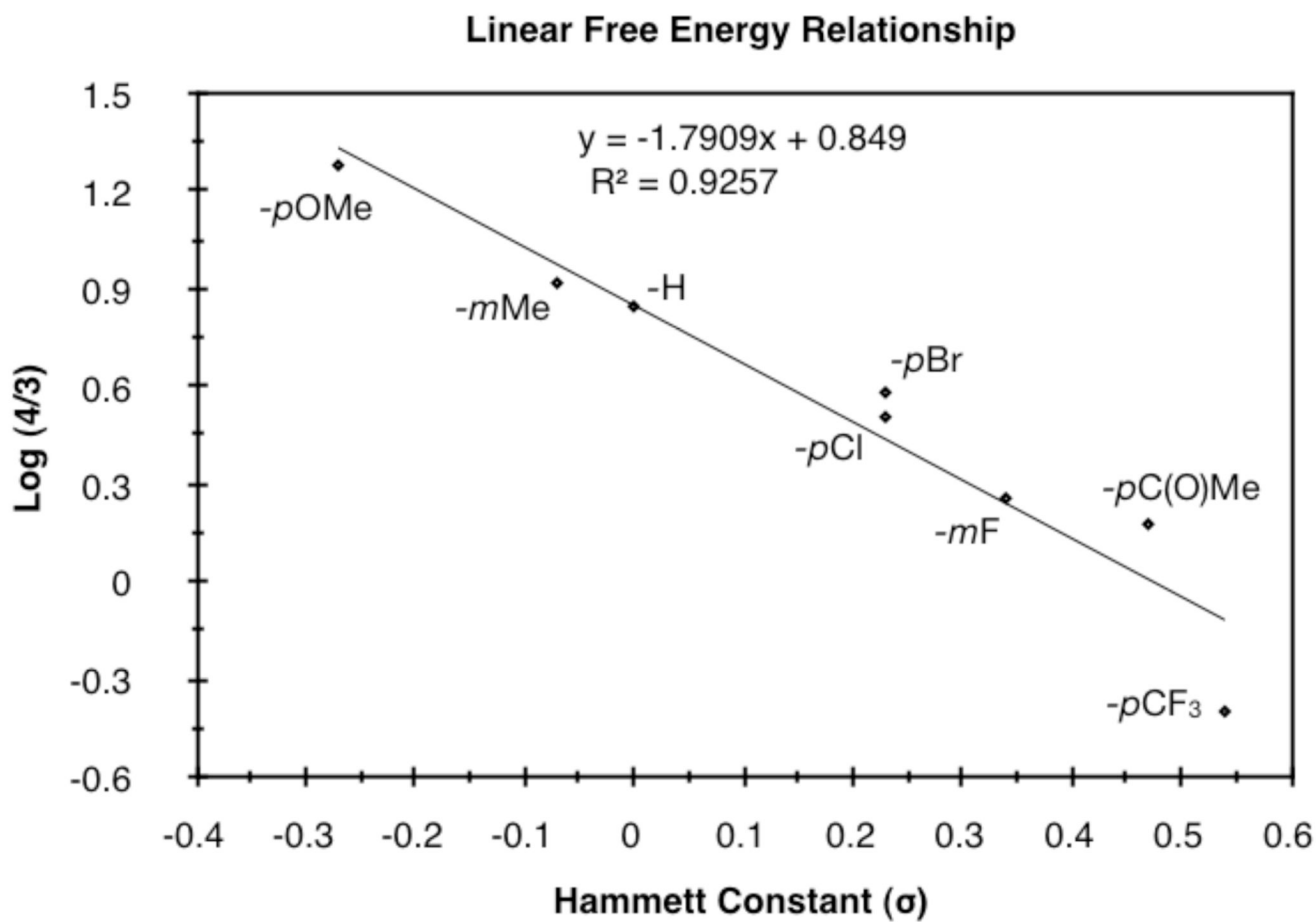


Figure 2.
Linear free energy relationship of aryl acetylenes.

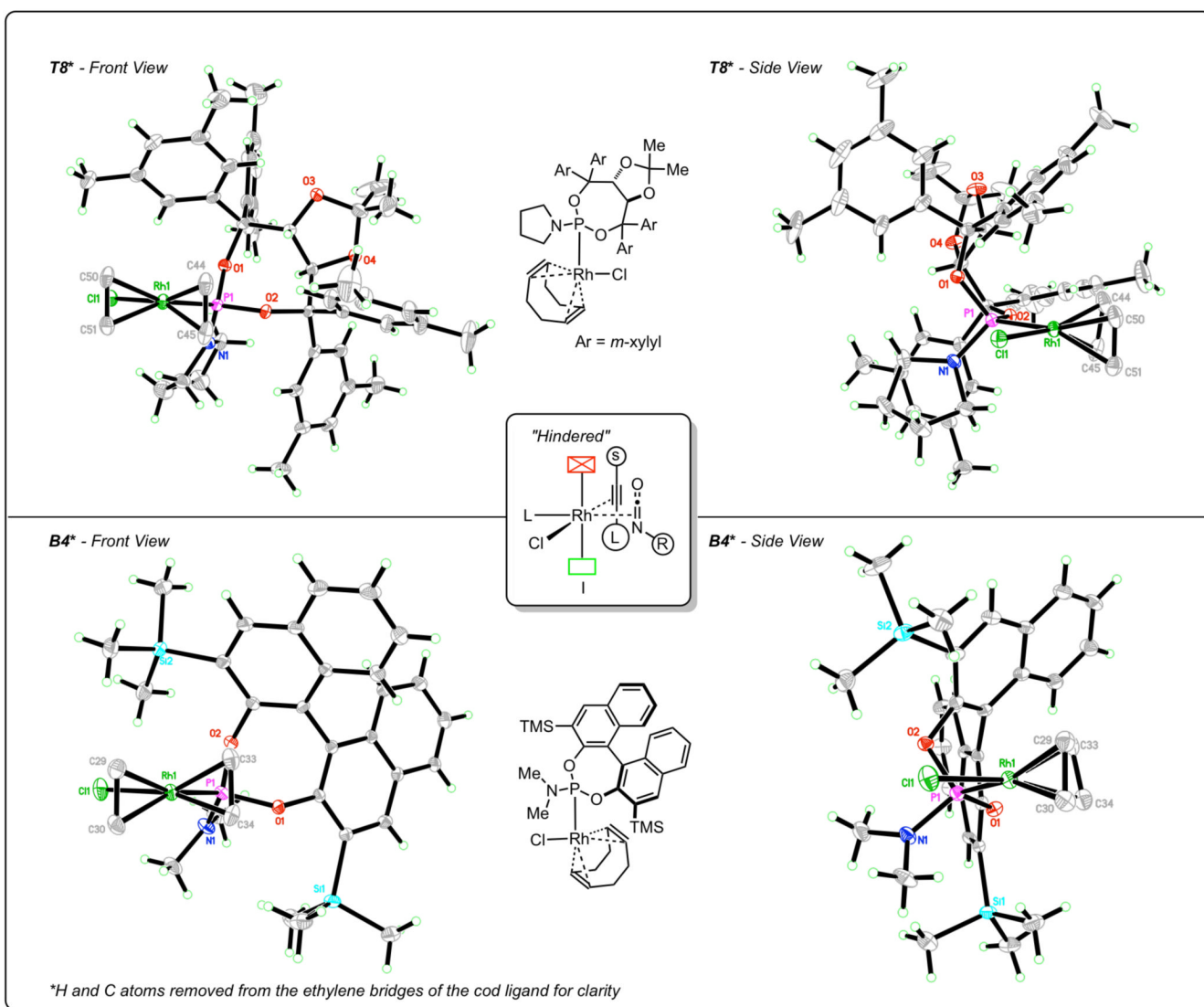
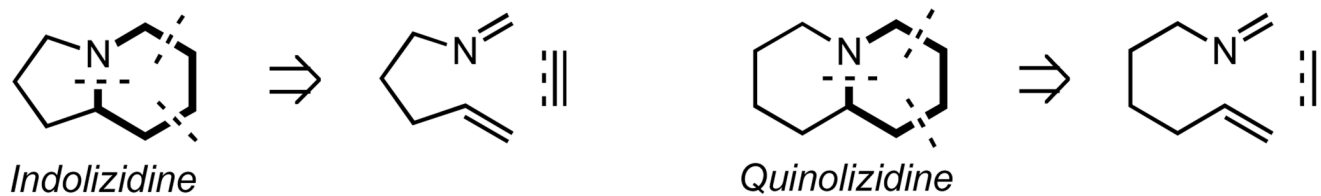
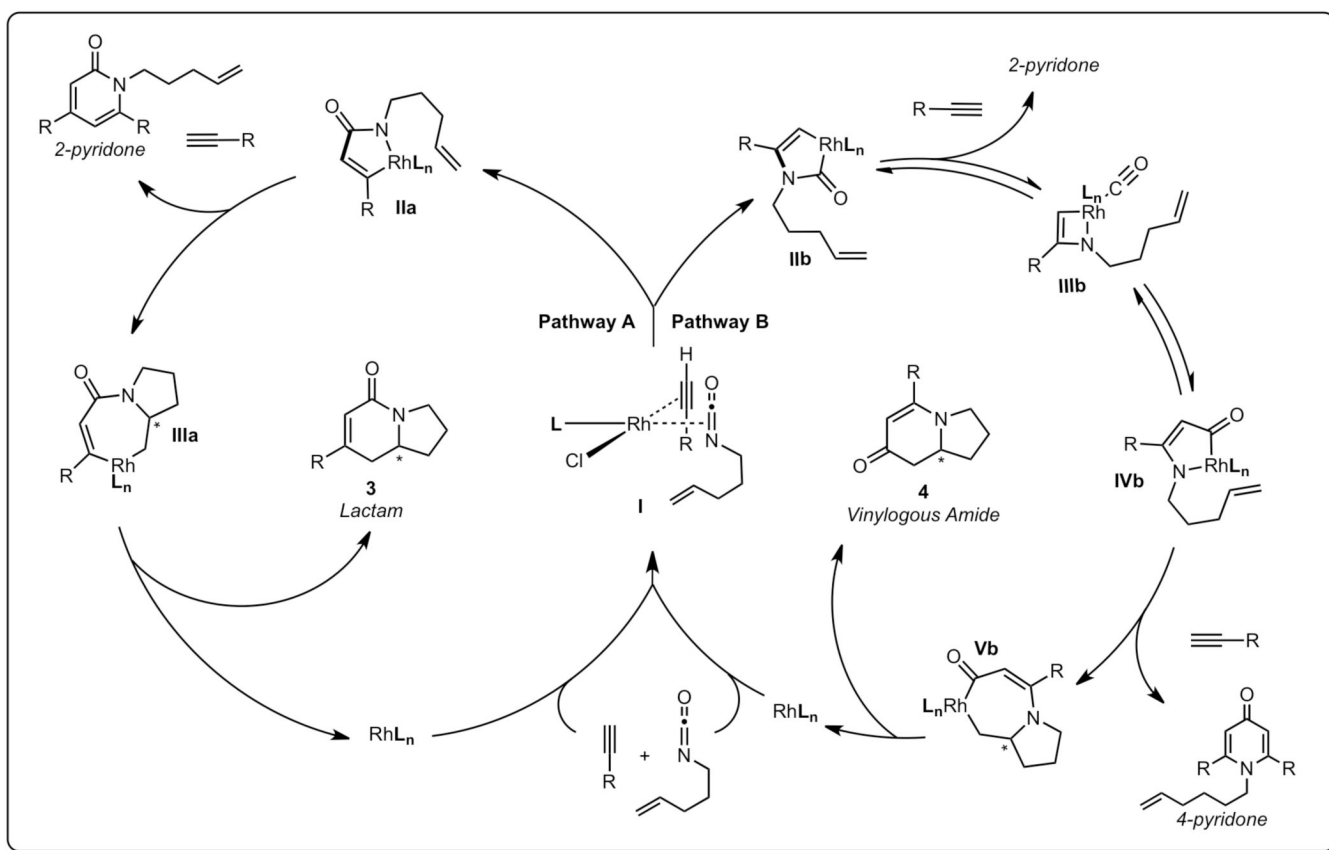


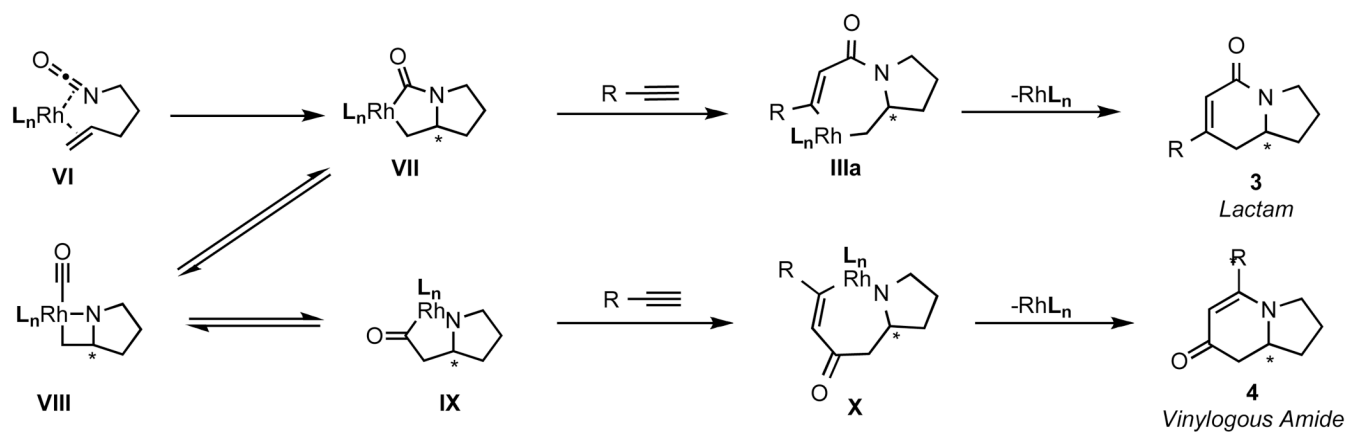
Figure 3.
X-ray crystal structures of Rh(cod)Cl/phosphoramidite complexes

**Scheme 1.**

[2+2+2] cycloadditions with alkynes and isocyanates.

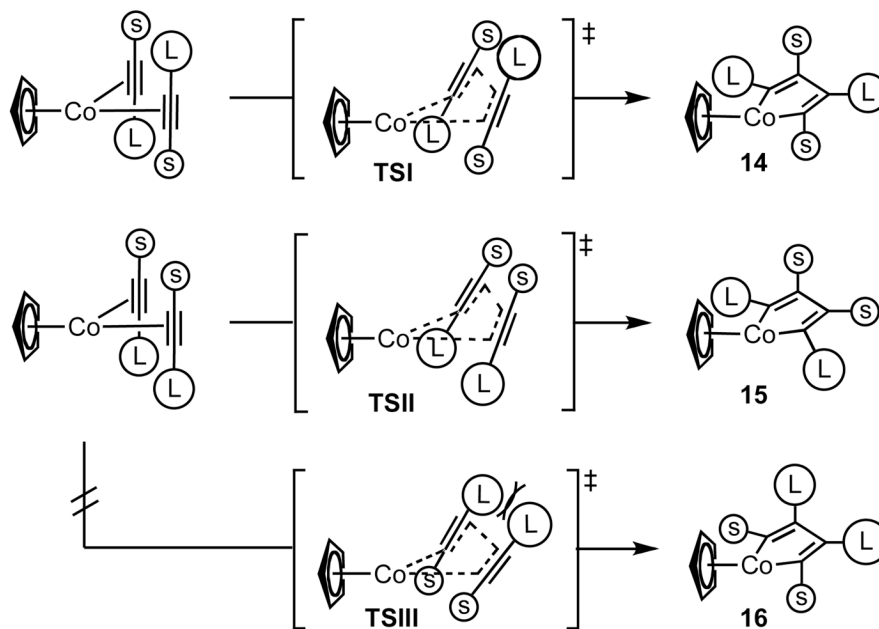
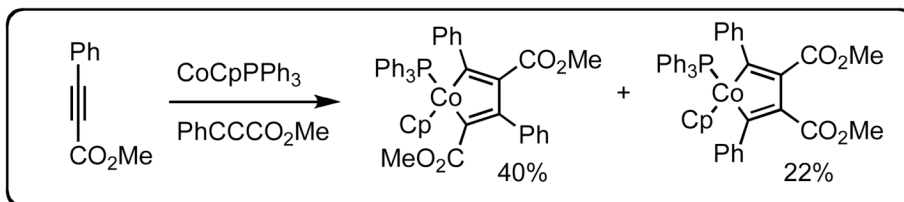


Scheme 2.
Proposed catalytic cycle.

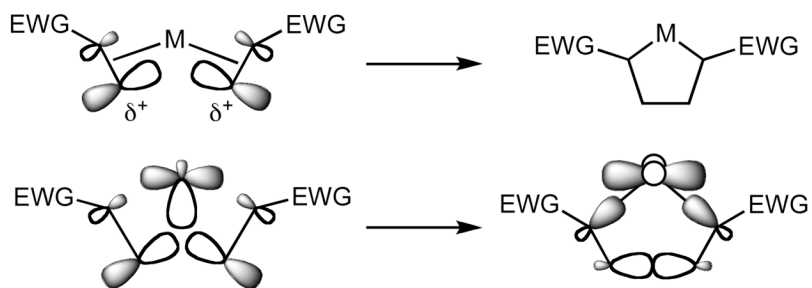


Scheme 3.
Alternative catalytic cycle

Wakatsuki and Yamazaki

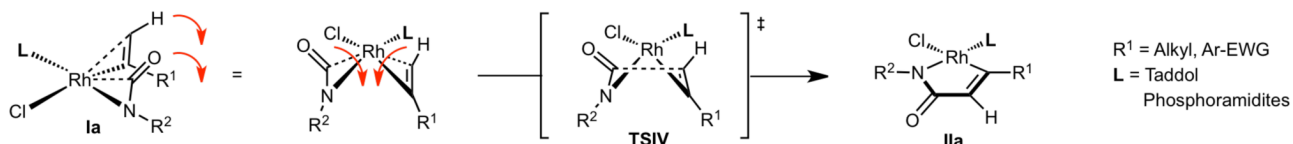


Stockis and Hoffmann

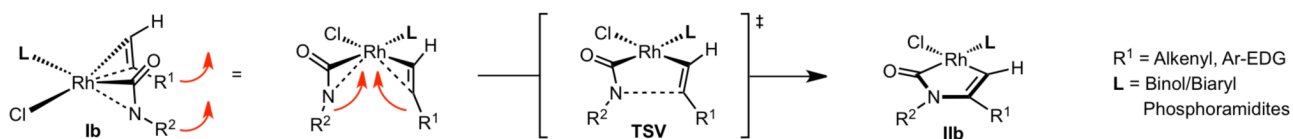
Largest LUMO coefficients prefer to be β to the metal

Scheme 4.
Regioselectivity models for metallacycle formation.

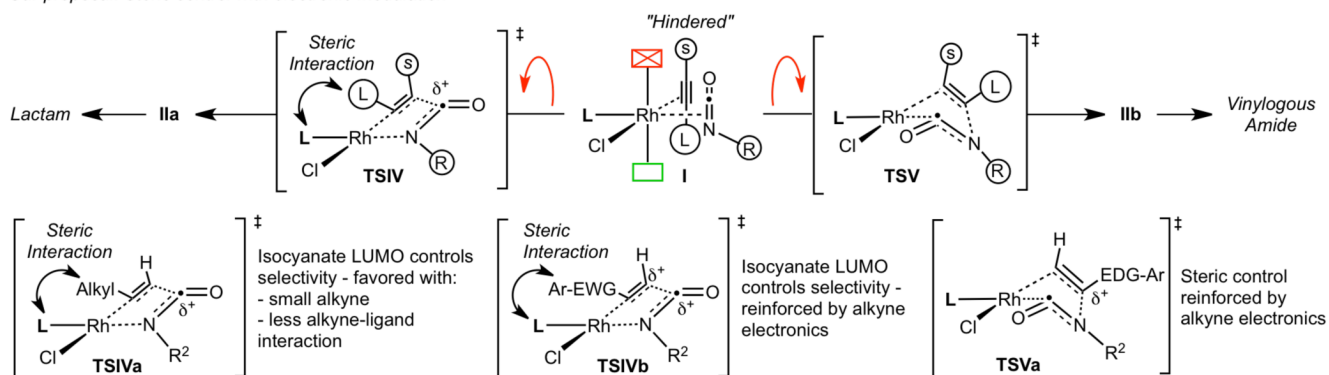
Lactam



Vinylogous Amide



Our proposal: Steric control with electronic modulation



Scheme 5.
Model to rationalize product selectivity.

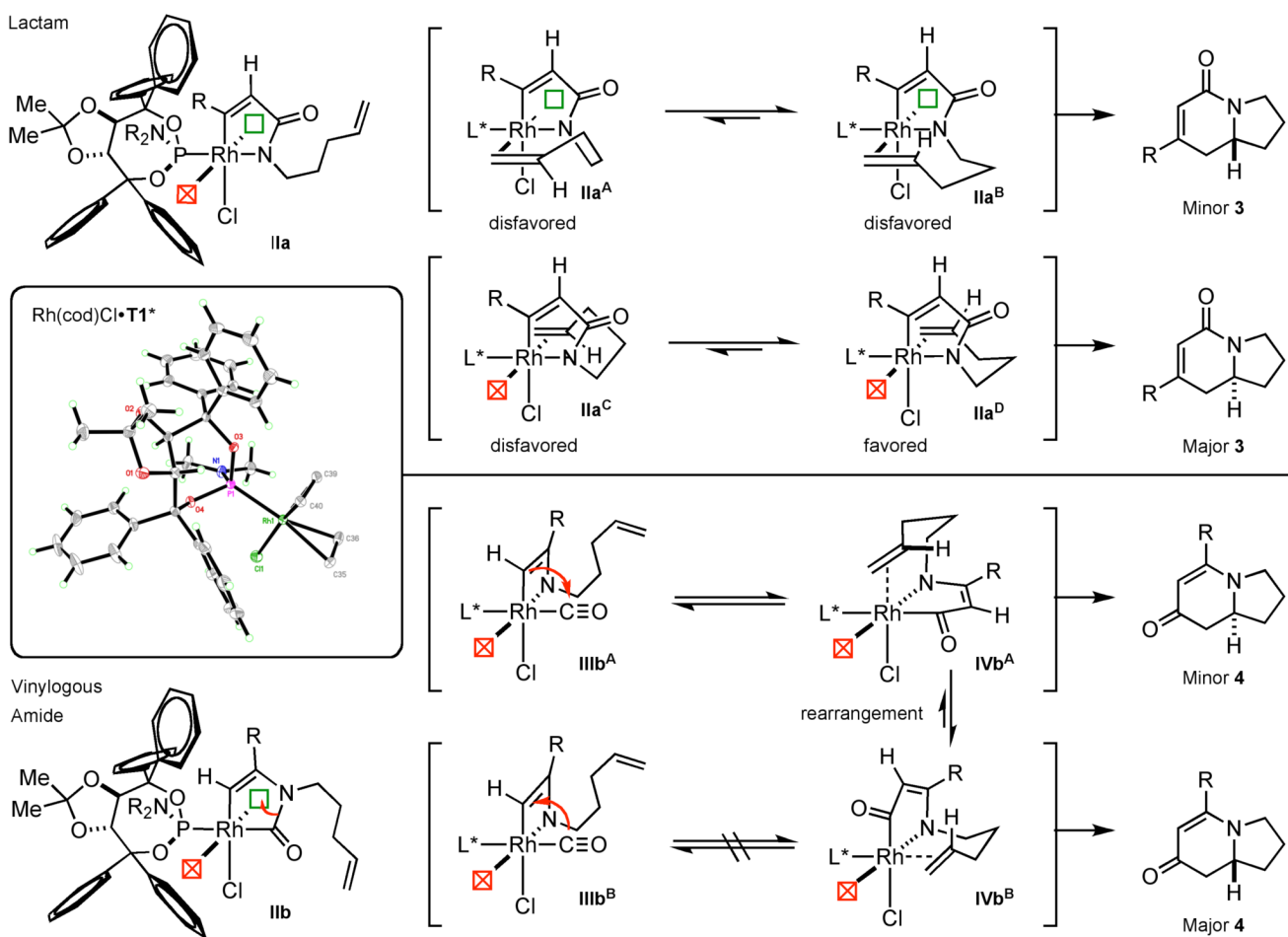
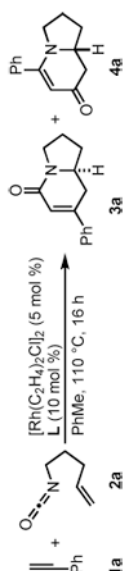


Table 1

Initial ligand screen.^a



entry	L	3a:4a ^b	yield (%) ^c	ee (%) ^d 3a	ee (%) ^d 4a
1	P(4-MeO-C ₆ H ₄) ₃	1:1	<20	-	-
2	BINAP	-	NR	-	-
3	dppb	>20:1	<5	-	-
4	B1	1:2.2	32	5 ^e	55 ^e
5	B2	1:4.5	50	45	8
6	B3	1:2.7	26	5 ^e	45 ^e
7	T1	1:7.0	80	83	94
8	T2	1:7.3	87	89	94
9	T3	1:3.3	76	90	81

^a Reaction conditions: **1** (2 equiv), **2**, [Rh(C₂H₄)₂Cl]₂ 5 mol %, **L** 10 mol % in PhMe at 110 °C for 16 h.

^b Ratio determined by ¹H NMR of crude reaction.

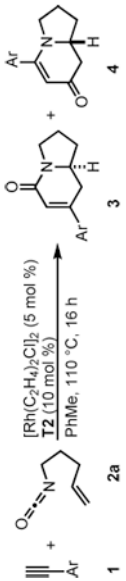
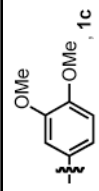
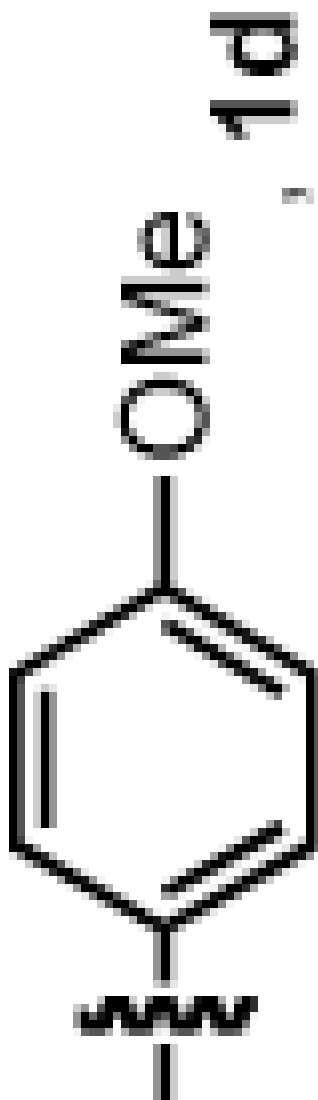
^c Combined isolated yield.

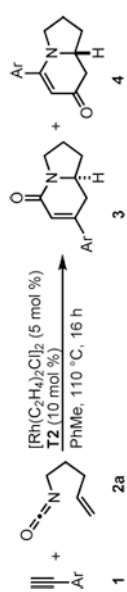
^d Determined by HPLC analysis on a chiral stationary phase.

^e Opposite enantiomer.

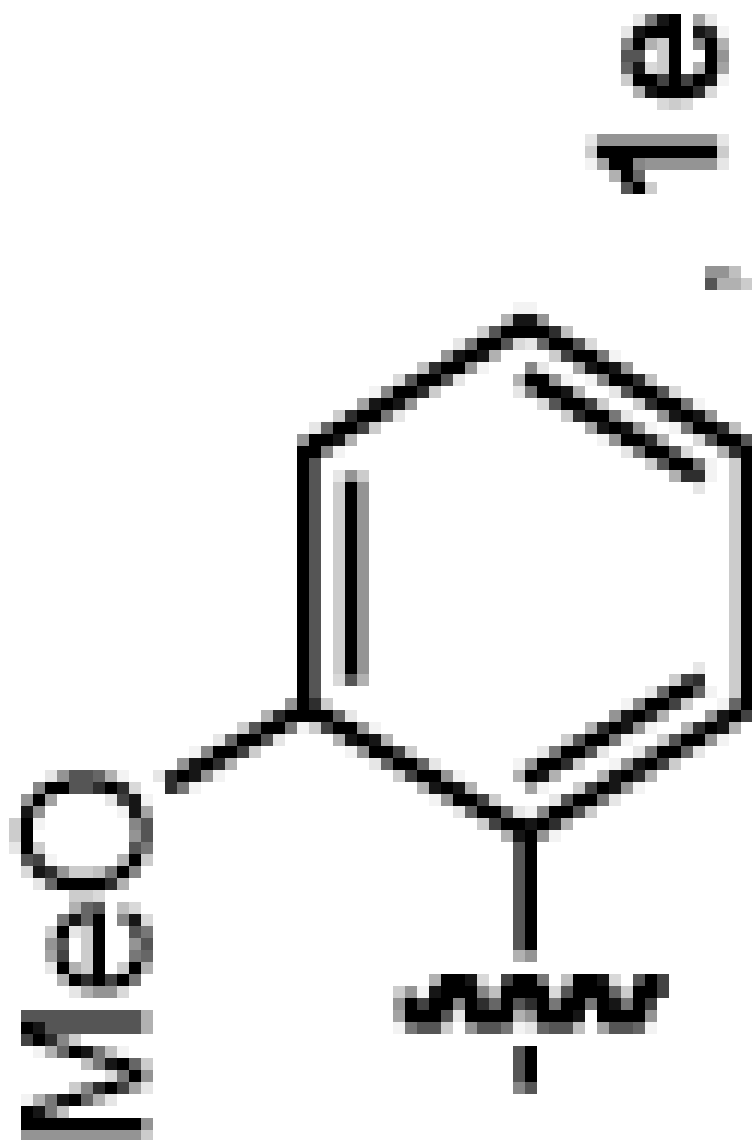
Table 2

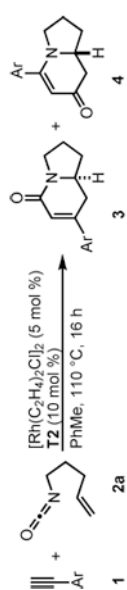
Terminal aryl alkynes scope.^a

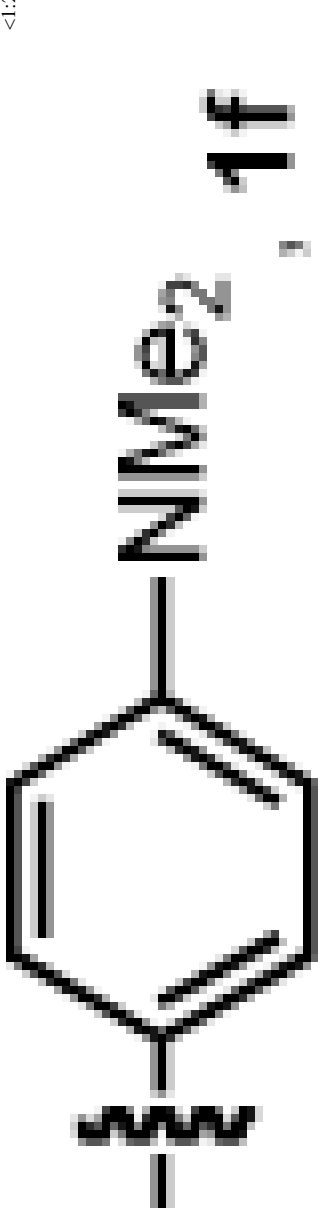
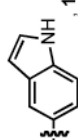
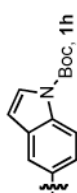
					
entry	Ar	3:4 ^b	yield (%) ^c	ee (%) ^{3d}	ee (%) ^{4d}
1		<1:20	72	-	94
2		<1:20	70	-	90



entry	Ar	3:4 ^b	yield (%) ^c	ee (%) ^{3d}	ee (%) ^{4d}
3		<1:20	64	-	94

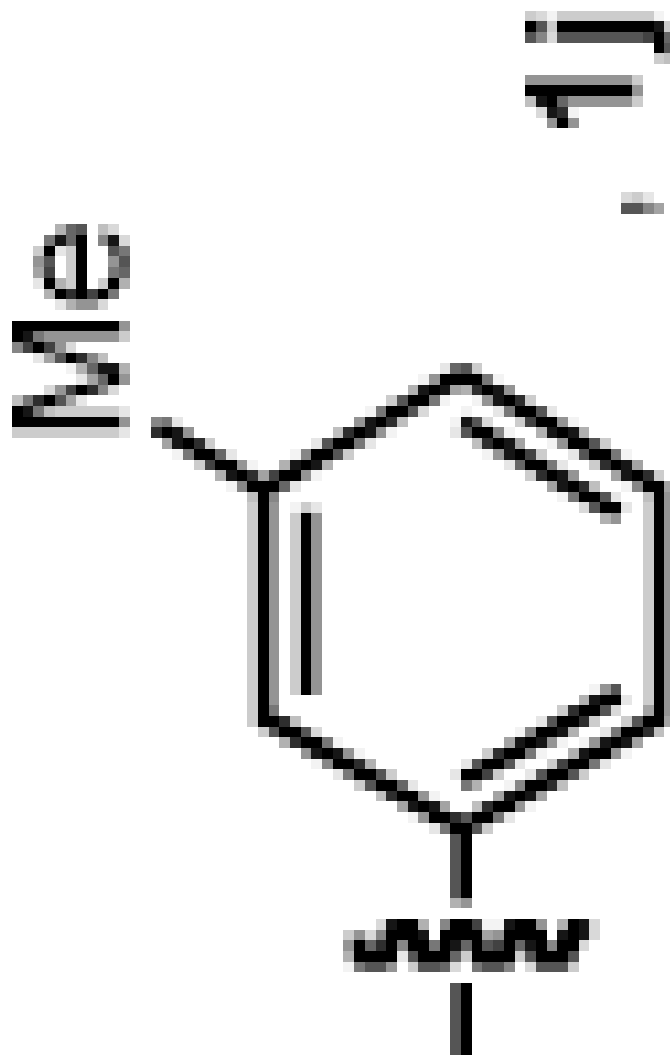
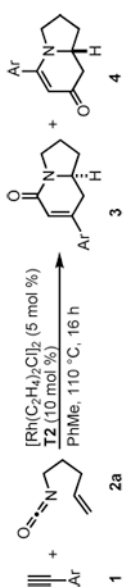


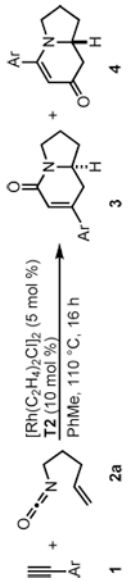

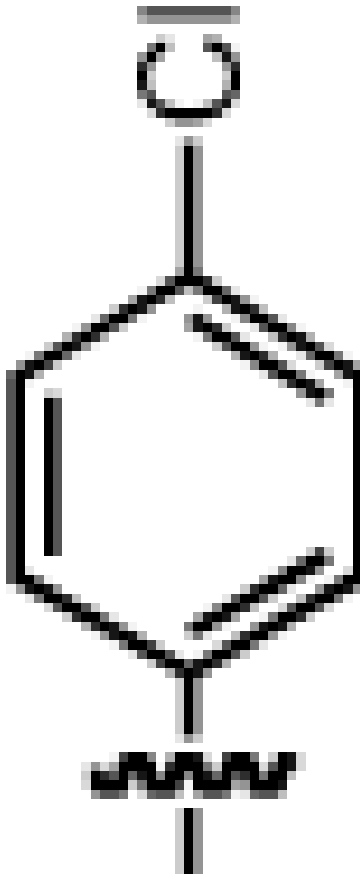


entry	Ar	3:4 ^b	yield (%) ^c	ee (%) ^{3d}	ee (%) ^{4d}
4		<1:20	78	-	87
5	 , 1g	<1:20	65	-	90
6	 , 1h	<1:20	85	-	91

entry	Ar	3:4 ^b	yield (%) ^c	ee (%) ^{3d}	ee (%) ^{4d}
1		1:9.0	64	-	86

entry	Ar	3:4 ^b		yield (%) ^c	ee (%) ^{3d}	ee (%) ^{4d}
		1:8.3				
8				65	-	94



							
entry	Ar	3:4 ^b	yield (%) ^c	ee (%) ^{3d}	ee (%) ^{4d}		
9		1:7.3	86	89		94	
10		1:3.8	65	93		91	

entry	Ar	3:4 ^b	yield (%) ^c	ee (%) ^{3d}	ee (%) ^{4d}
11		1:3.2	72	90	89
12		1:1.8	68	94	94
13		1:1.5	65	94	81
14		2.5:1	50	94	-

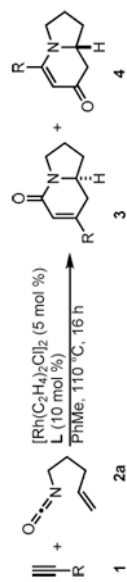
entry	Ar	3:4 ^b	yield (%) ^c	ee (%) ^{3d}	ee (%) ^{4d}
15		<1:20	96	-	92

^dSee Table 1.
^dT3 used as ligand.

Table 3

Scope of alkyl alkynes.^a

entry	R	T3			A1f		
		3:4 ^b	yield (%) ^c	ee (%) ^c	3:4 ^b	yield (%) ^c	ee (%) ^d
1	<i>n</i> -hex, 1q	5.0:1	78	80/33	1:6.0	66	91 ^e
2	(CH ₂) ₄ CO ₂ Me, 1r	5.8:1	65	80/-	1:5.0	66	90 ^e
3	(CH ₂) ₂ Ph, 1b	>20:1	47	84/-	1:5.0	56	91 ^e
4	Bn, 1s	>20:1	50	84/-	1:3.0	52	90 ^e
5	(CH ₂) ₂ OTf, 1t	>20:1	65	87/-			
6	(CH ₂) ₄ OTf, 1u				1:5.0	62	90 ^e
7	CH ₂ OMe, 1v	>20:1	46	76/-			
8	Cy, 1w	1.2:1 ⁸	82 ⁸	77/95 ⁸	1:14	86	91 ^e
9	(CH ₂) ₄ Cl, 1x				1:5.0	57	94 ^e
10	(CH ₂) ₄ CCl, 1y				1:7.2	60	90 ^e
11	(CH ₂) ₃ CCl, 1z				1:5.0	55	91 ^e
12	<i>t</i> -Bu, 1aa				1:10	67	79 ^e

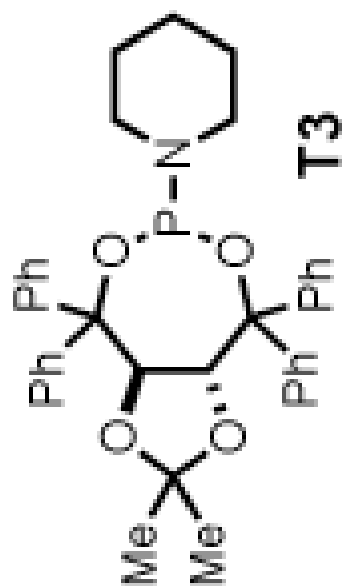
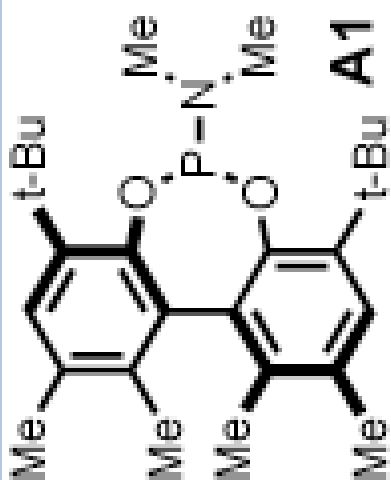


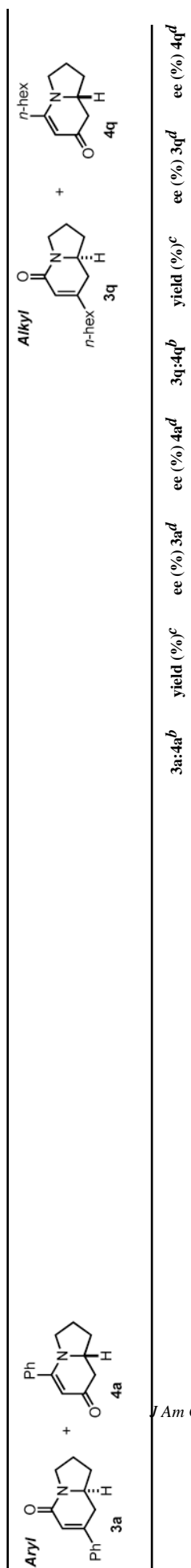
entry	R	T3			A1f		
		3:4 ^b	yield (%) ^c	ee (%) ^d	3:4 ^b	yield (%) ^c	ee (%) ^d
13		1:5	54	90 ^e			

^eSee Table 1.

Reaction conditions: **1** (2 equiv), **2a**, $[\text{Rh}(\text{C}_2\text{H}_4)_2\text{Cl}]_2$ 2.5 mol %, **L** 5 mol % in PhMe at 110 °C for 16h.

11 used as ligand.



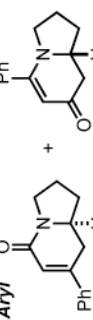



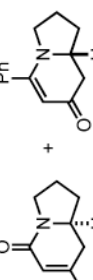
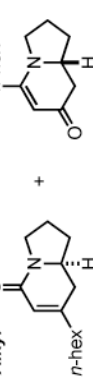
3a:4a^b	yield (%)^c	ee (%) 3a^d	ee (%) 4a^d	3q:4q^b	yield (%)^c	ee (%) 3q^d	ee (%) 4q^d
1:7.0	80 ^f	83	94	3.2:1	81 ^f	81	73

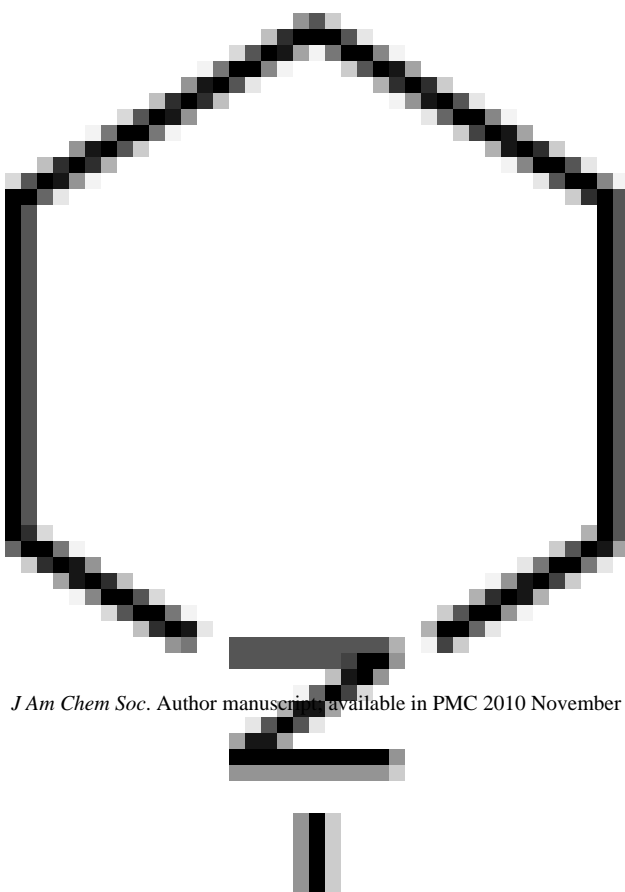
		3a:4a ^b	yield (%) ^c	ee (%) 3a ^d	ee (%) 4a ^d	3q:4q ^b	yield (%) ^c	ee (%) 3q ^d	ee (%) 4q ^d		
		1:7.3	87 ^f	89	94	2.4:1	80 ^f	83	70		
										1:3.3	76 ^f
										5.0:1	78 ^f
										81	80
										33	

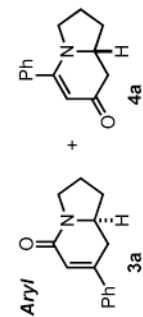
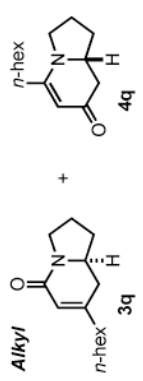
Aryl		Alkyl		3a:4a ^b	yield (%) ^c	ee (%) 3a ^d	ee (%) 4a ^d	3q:4q ^b	yield (%) ^c	ee (%) 3q ^d	ee (%) 4q ^d
				1:2.0	14	-	-	>20:1	5	-	-

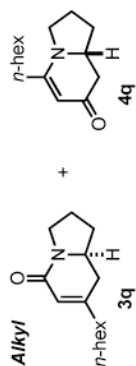
		3a:4a ^b	yield (%) ^c	ee (%) 3a ^d	ee (%) 4a ^d	3q:4q ^b	yield (%) ^c	ee (%) 3q ^d	ee (%) 4q ^d		
		1:6.5	84	91	95	2.5:1	55	87	76		

 <p>Aryl + 3a → 4a</p>	 <p>Alkyl + 3q → 4q</p>					
3a:4a^b 1:2.8	yield (%)^c 68	ee (%)^d 87	3q:4q^b 8.3:1	yield (%)^c 68	ee (%)^d 83	ee (%)^d 46

									
		3a:4a ^b	yield (%) ^c	ee (%) 3a ^d	ee (%) 4a ^d	3q:4q ^b	yield (%) ^c	ee (%) 3q ^d	ee (%) 4q ^d
		1:>20	67	69	84	1:1	31	79	74



											
3a:4a ^b	yield (%) ^c	ee (%) ^d	3q:4q ^b	yield (%) ^c	ee (%) ^d	3q:4q ^b	yield (%) ^c	ee (%) ^d	3q:4q ^b	yield (%) ^c	ee (%) ^d
1:5.6	84	96	4.0:1	77	90	74					
1:1.6	75	94	12.5:1	72	82	51					
1:2.2	32 ^f	5	1:1.9	19	14 ^e	67 ^e					
1:4.5	50 ^f	45 ^e	1:4.2	34	18	59					



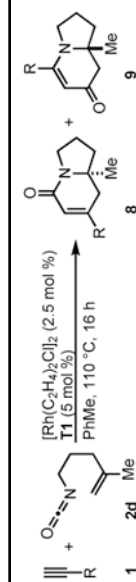
$3a:4a^b$	yield (%) ^c	ee (%) $3a^d$	ee (%) $4a^d$	$3q:4q^b$	yield (%) ^c	ee (%) $3q^d$	ee (%) $4q^d$
1:7.1	74	36	45 ^e	1:3.6	53	32 ^e	95 ^e
1:12.5	77	37	55 ^e	1:3.6	51	50 ^e	95 ^e
1:12	82	43	55 ^e	1:3.2	63	47 ^e	92 ^e
1:>20	77	41	3 ^e	1:6.2	75	8	91 ^e

^ν See Table 1.

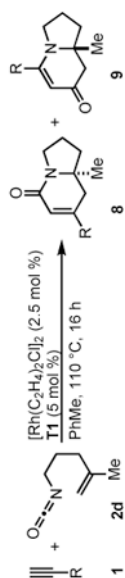
^f Reaction conditions: **1** (2 equiv), **2a**, [Rh(C₂H₄)₂Cl]₂ 5 mol %, **L** 10 mol % in PhMe at 110 °C for 16 h.

Table 5

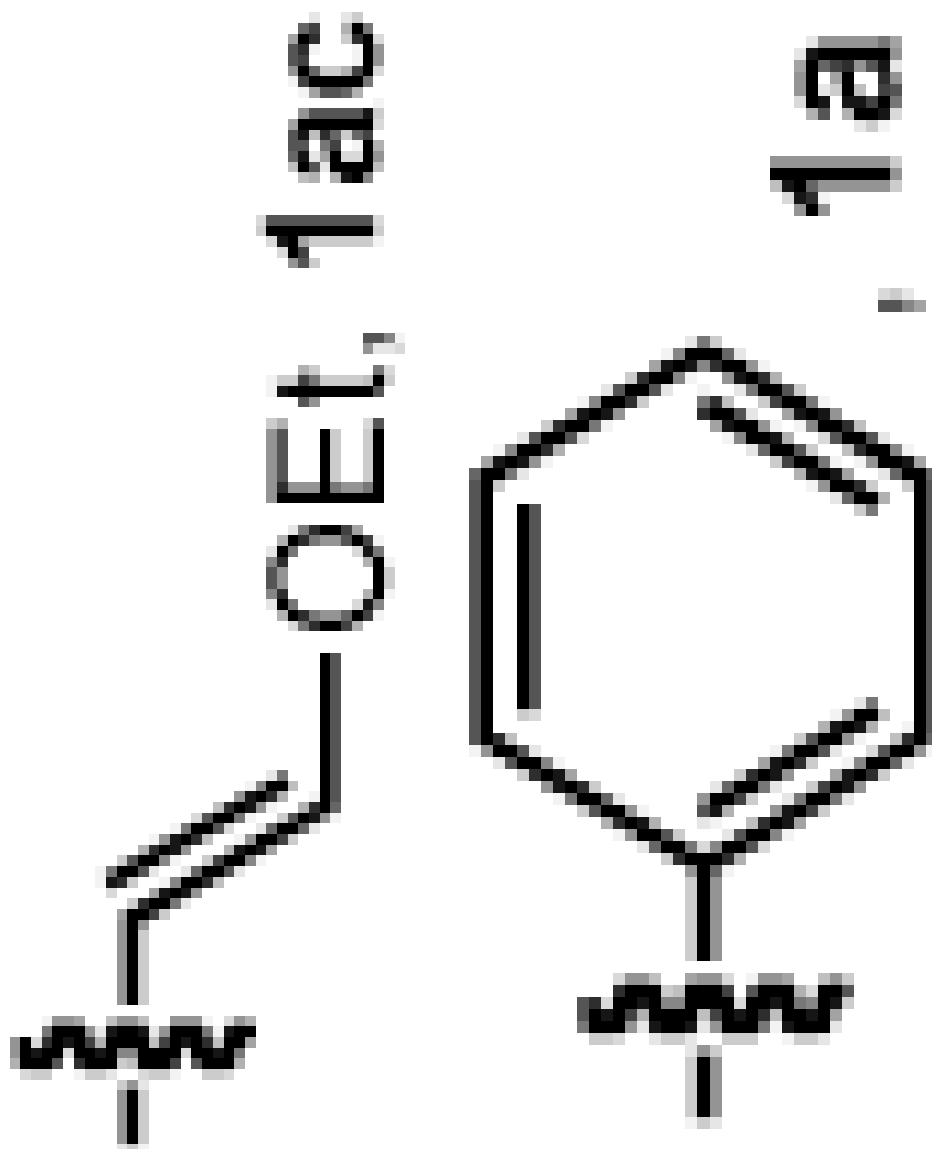
Conjugated alkynes with 1,1-disubstituted alkenyl isocyanates.^a

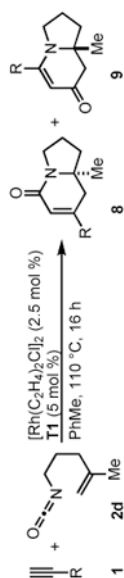


entry	R	8:9 ^b	yield (%) ^c	ee (%) ^d	ee (%) ^d
1		< 1:20	80	-	91
2		1:9	84	-	91



entry	R	8:9 ^b	yield (%) ^c	ee (%) ^{8d}	ee (%) ^{9d}
3		1:9	64	-	91



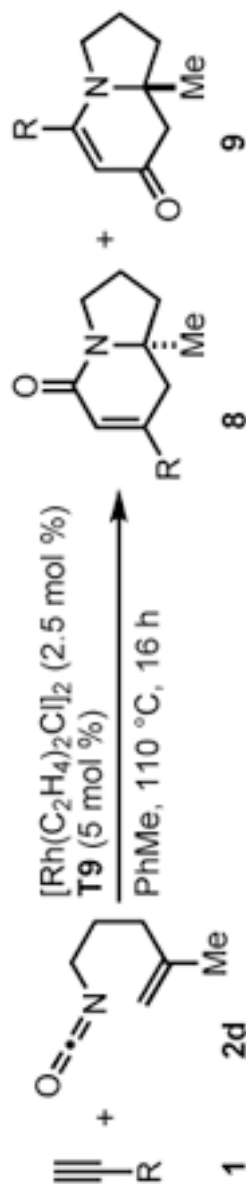


entry	R	8: ^b	yield (%) ^c	ee (%) ^d	ee (%) ^d
5		1:8	85	-	91
6		1:8	78	-	83
7		1:3	77	82	88

^aSee Table 4.

^{b-d}See Table 1.

Table 6

Alkyl alkynes with 1,1-disubstituted alkenyl isocyanates.^a


entry	R	8: ^b	yield (%) ^c	ee (%) ^{8d}	ee (%) ^{9d}
1	<i>n</i> -hex, 1q	6.5:1	88	91	56
2	(CH ₂) ₄ CO ₂ Me, 1r	8:1	83	93	49
3	(CH ₂) ₂ Ph, 1b	9.5:1	71	95	-
4	Bn, 1s	13:1	71	9-	-
5	(CH ₂) ₂ OTBS, 1t	11.5:1	77	93	-
6	(CH ₂) ₃ OTBS, 1ad	9:1	70	95	64
7	(CH ₂) ₄ Cl, 1x	8:1	60	91	-
8	(CH ₂) ₃ CCTMS, 1ae	6:1	45	93	85

^aSee Table 4.^{b-d}See Table 1.

Table 7

Scope of 1,1-disubstituted alkenyl isocyanates.

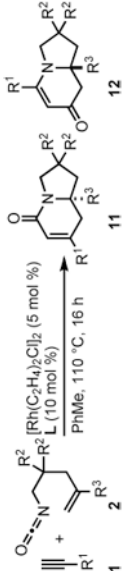
Reaction scheme showing the cyclization of an alkyne (**1c**) and an alkenyl isocyanate (**2**) to form a bicyclic product (**10**). The reaction conditions are $[\text{Rh}(\text{C}_2\text{H}_4)_2\text{Cl}]_2$ (2.5 mol %), **T1** (5 mol %), PhMe, 110 °C, 16 h. The aryl group Ar is defined as 4-MeO-C₆H₄.

entry	R	yield (%) ^c	ee (%) 10 ^d
1	<i>n</i> -Bu, 2e	71	90
2	<i>i</i> -Bu, 2f	75	94
3	Bn, 2g	80	92
4	(CH ₂) ₂ <i>i</i> -Pr, 2h	83	91
5	(CH ₂) ₂ Ph, 2i	80	90
6	<i>i</i> -Pr, 2j	50	89
7	Cy, 2k	19	86
8	CH ₂ OCH ₂ Ph, 2l	77	92
9	(CH ₂) ₄ OTBS, 2m	74	88
10	(CH ₂) ₄ Cl, 2n	63	90
11	(CH ₂) ₂ CH=CH ₂ , 2o	75	91

^a See Table 4.^{b,d} See Table 1.^c Isolated yield.

Table 8

Substitution on the alkyl tether.^a

						
entry	L	R ¹	R ²	R ³	11:12 ^b	yield (%) ^c
1	T1	4-MeO-C ₆ H ₄	CO ₂ Et	H, 2p	1:15	88
2	B4	4-MeO-C ₆ H ₄	CO ₂ Et	H, 2p	1:1	69
3	T1	4-MeO-C ₆ H ₄	Me	H, 2q	1:>20	72
4	B4	4-MeO-C ₆ H ₄	Me	H, 2q	1:5.0	62
5	B4	PMB, 1af	Me	Me, 2r	1:2.2	65
6	A1	PMB, 1af	Me	Me, 2r	1:4.0	72
						ee (%) 11/12 ^d
						74/91
						<5/16 ^e
						-/83
						-/30 ^e
						52/94 ^e
						56/82 ^e

^{a-e}See Table 1.

^fReaction conditions: **1** (2 eq), **2**, [Rh(C₂H₄)₂Cl]₂ 2.5 mol %, **L** 5 mol % in PhMe at 110 °C for 16 h.

Table 9

Selected bond lengths of rhodium(I)(cod)chloride/phosphoramidite complexes.

Ligand	Trans to P				Trans to Cl	
	Rh-P	Rh-Cl	Rh-C=C*	C=C	Rh-C=C*	C=C
T9	2.2703(4)	2.3654(4)	2.132	1.409(2)	1.994	1.413(3)
T8	2.2688(6)	2.3765(6)	2.131	1.377(4)	1.992	1.395(4)
T1	2.2648(6)	2.3777(6)	2.140	1.376(4)	1.997	1.417(3)
T2	2.2547(3)	2.3842(3)	2.152	1.3781(18)	1.995	1.4131(16)
A1	2.2451(4)	2.3485(4)	2.162	1.369(3)	2.013	1.409(2)
B4	2.2388(9)	2.3455(8)	2.151	1.365(5)	2.003	1.396(5)

* Bond length from Rh to centroid of alkene

